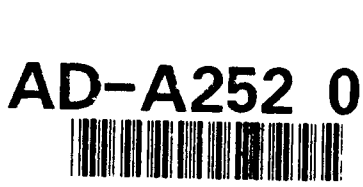

Report CITLL-92-01

COUPLED WAVEGUIDE GAS LASER RESEARCH

William B. Bridges, Yongfang Zhang, and Reynold E. Johnson

California Institute of Technology

Pasadena, California 91125

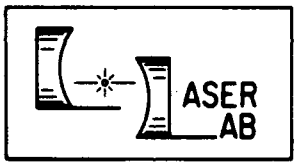

15 May 1992

Final Report for Period 1 January 1988 - 30 June 1991

Approved for public release; distribution unlimited

Prepared for:

AIR FORCE OFFICE OF SCIENTIFIC RESEARCH

Air Force Systems Command

Bolling Air Force Base, D.C. 20332-6448

SECURITY CLASSIFICATION OF THIS PAGE

REPORT DOCUMENTATION PAGE

1a. REPORT SECURITY CLASSIFICATION: UNCLASSIFIED	1b. RESTRICTIVE MARKINGS
2a. SECURITY CLASSIFICATION AUTHORITY	3. DISTRIBUTION / AVAILABILITY OF REPORT: Approved for public release, distribution unlimited.
2b. DECLASSIFICATION / DOWNGRADING SCHEDULE	
4. PERFORMING ORGANIZATION REPORT NUMBER(S): CITLL-92-01	5. MONITORING ORGANIZATION REPORT NUMBER(S)
6a. NAME OF PERFORMING ORGANIZATION: California Institute of Technology; 6b. OFFICE SYMBOL (If applicable)	7a. NAME OF MONITORING ORGANIZATION: Air Force Office of Scientific Research
6c. ADDRESS (City, State, and ZIP Code): Pasadena, California 91125	7b. ADDRESS (City, State, and ZIP Code): Bolling AFB, DC, 20332-6448
8a. NAME OF FUNDING / SPONSORING ORGANIZATION: AFOSR; 8b. OFFICE SYMBOL (If applicable): NE	9. PROCUREMENT INSTRUMENT IDENTIFICATION NUMBER: AFOSR-88-0085
8c. ADDRESS (City, State, and ZIP Code): Bolling AFB, DC, 20332-6448	10. SOURCE OF FUNDING NUMBERS: PROGRAM ELEMENT NO. 61102; PROJECT NO. 2301; TASK NO. A5; WORK UNIT ACCESSION NO.
11. TITLE (Include Security Classification): Coupled Waveguide Gas Laser Research (unclassified)	
12. PERSONAL AUTHOR(S): Bridges, William B.; Zhang, Yongfang; and Johnson, Reynold E.	
13a. TYPE OF REPORT: Final; 13b. TIME COVERED: FROM 88-1-1 TO 91-6-30; 14. DATE OF REPORT (Year, Month, Day): 1992, May 15; 15. PAGE COUNT: 74	
16. SUPPLEMENTARY NOTATION	

17. COSATI CODES			18. SUBJECT TERMS (Continue on reverse if necessary and identify by block number)
FIELD	GROUP	SUB-GROUP	CO_2 waveguide lasers; coupled waveguide lasers; dielectric coated waveguides; r-f excited CO_2 lasers; parallel-plate waveguide lasers.

19. ABSTRACT (Continue on reverse if necessary and identify by block number)

The overall objectives of this program were to study and develop an understanding of the characteristics of coupled waveguide gas lasers and to improve their operating characteristics. A flexible test bed laser was designed, fabricated and used to evaluate both ceramic and metal waveguide array structures. The strong tendency to phase lock with adjacent channels out-of-phase was confirmed. Metal waveguide walls were shown to produce power output comparable to ceramic walls. A simple metal slab laser was demonstrated with good discharge and good mode characteristics, and an unstable resonator was used to produce the lowest order cosine-Gaussian mode. A technique of coupling discharge channels with slots in the slab waveguide walls was conceived and shown to lock all-in-phase perferentially over the out-of-phase configuration. A concept for an all-metal, low-cost, microwave-excited waveguide laser using either a simple slab waveguide or the slot coupled array was developed.

20. DISTRIBUTION / AVAILABILITY OF ABSTRACT: ☐ UNCLASSIFIED/UNLIMITED ☐ SAME AS RPT ☐ DTIC USERS	21. ABSTRACT SECURITY CLASSIFICATION: Unclassified
22a. NAME OF RESPONSIBLE INDIVIDUAL: Dr. Howard Schlossberg	22b. TELEPHONE (Include Area Code): (202) 767-4906; 22c. OFFICE SYMBOL: NE

DD FORM 1473, 84 MAR — 83 APR edition may be used until exhausted. All other editions are obsolete.

SECURITY CLASSIFICATION OF THIS PAGE: Unclassified

Report CITLL-92-01

COUPLED WAVEGUIDE GAS LASER RESEARCH

William B. Bridges, Yongfang Zhang, and Reynold E. Johnson

California Institute of Technology

Pasadena, California 91125

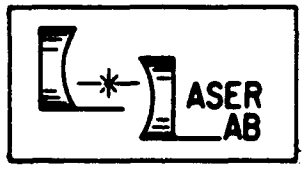

15 May 1992

Final Report for Period 1 January 1988 - 30 June 1991

Approved for public release; distribution unlimited

Prepared for:

AIR FORCE OFFICE OF SCIENTIFIC RESEARCH

Air Force Systems Command

Bolling Air Force Base, D.C. 20332-6448

SUMMARY

The overall objectives of this program were to study and develop an understanding of the characteristics of coupled waveguide gas lasers and to improve their operating characteristics if possible.

A flexible test bed laser was designed, fabricated, and used in a series of experiments on multiple bore waveguide laser arrays. These used both precision-ground ceramic arrays loaned by United Technologies Optical Systems (UTOS) and metal arrays fabricated at Caltech. We observed the strong tendency to lock in the out-of-phase configuration (highest order supermode) rather than the all-in-phase configuration (lowest order supermode), just as the UTOS work had shown. We demonstrated that simple slab waveguides could operate with good discharge uniformity and good mode quality, and that the lowest order cosine-Gaussian mode could be selected with an unstable resonator. We demonstrated that the slab guide walls could be simple bare metal or anodized metal, and still give comparable output power to ceramic array lasers, down to a separation of 1 to 1.5 mm, thus offering an attractive alternative to the more complex arrays. We conceived and developed a novel structure consisting of an array coupled by intervening slots rather than intervening walls, and demonstrated that in this structure the all-in-phase array mode is favored over the out-of-phase mode. We conceived a novel all-metal structure that incorporates the metal slab optical waveguide with a microwave ridge waveguide, and uses an inexpensive oven magnetron at 2450 MHz as the power source. This structure should operate with cosine-Gaussian modes in the simple slab configuration, or as an all-in-phase array with the slot-couple array concept. Unfortunately, the present contract ended before this laser concept could be demonstrated experimentally.

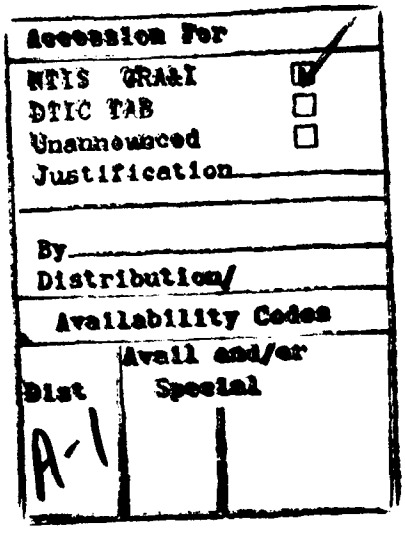

PROGRAM OBJECTIVES

The original objectives of this program are to study and develop an understanding of the characteristics of coupled waveguide gas lasers and to improve the operating characteristics if possible. The work is both experimental and theoretical.

The plan of attack outlined in the proposal included the following elements on the experimental side:

- Design and fabricate a flexible CO_2 waveguide laser test bed compatible in dimensions with the waveguide ceramic sections fabricated by the group at United Technologies Optical Systems (UTOS).

- Calibrate the performance of the system against the UTOS work by running UTOS-supplied ceramic sections in our system.

- Following the calibration runs, execute a set of experiments designed to study the important properties of waveguide array supermodes. This would include sensitivity to the waveguide parameters (such as waveguide dimensions, coupling method and dimensions, mirror alignment, etc.)

- Following the parametric studies, execute a set of experiments designed to explore the new ideas described in the proposal: the alternate-guide output mirror, and periodic coupling along the guide. Needless to say, the experiments should include any further promising new ideas that come to light, either through our own work or the work of others.

- In parallel with these experiments, explore the use of new materials for the coupled waveguide arrays that would have better performance or easier and less expensive fabrication.

On the theoretical side, we proposed to develop a coupled-mode theory sufficiently detailed to allow comparison with both the parametric measurements and the proposed new experiments with special mirror, periodic coupling, etc.

During the final year of the program suggested a new objective: Development of an all-metal, microwave-excited laser using planar electrodes which also served as waveguides in one dimension (a "slab laser".) While we were not able to realize this goal during the contract period, we have continued work on this project with promising results through the present time.

REVIEW OF PREVIOUS TWO YEARS RESULTS

A. PRELIMINARY EXPERIMENTS WITH METAL WAVEGUIDES.

At the very outset of this program, it became apparent through discussions with the UTOS personnel and with ceramic vendors, that the cost of precision-ground, multiple-waveguide ceramic pieces was going to be very high. By the time we began the program, UTOS had already decided that the cost was so high (the order of $1000 per piece) that they chose to buy the precision grinding equipment ($50,000) and train a UTOS technician to run it. We did not have the option to do the same. Richard Hart at UTOS was kind enough to loan us some of their precision ceramics to serve as calibration standards for our test bed (see Section C), but we could not ask UTOS to fabricate special pieces for our experiments. We needed to be able to pursue our own ideas, but without the extreme cost of precision grinding, so we explored a possible alternative: making the complicated multiple waveguide pieces out of aluminum and then anodizing it to make the surface look like aluminum oxide, the same as the ceramic.

In retrospect, what seemed as a problem at the time has resulted, fortuitously, in an advantage: Not only were we able to make the complicated waveguide structures much more inexpensively in aluminum than ceramic and have them behave substantially the same, but our work eventually led to a much more practical structure for the laser, as we will describe in later sections. However, in 1988 it was not obvious that a machined aluminum structure would even support an appropriate discharge, much less provide a comparable output power. Figure 1, taken from our first annual report[1], shows the first discharges in a metal waveguide structure in a non-laser bell-jar test. We were encouraged by the fact that the discharge seemed to be essentially the same as that obtained with similarly shaped ceramic pieces. And it was the same whether the aluminum pieces were anodized or not.

B. THEORY OF LOSSES IN METAL AND DIELECTRIC COATED METAL WAVEGUIDES.

Of course, just having a good discharge in the laser region is not enough; there remained the question of the optical losses in the metal or dielectric-coated metal waveguides. Common wisdom in the 1970's seemed to indicate that "metal wall losses would be too great at 10 microns to make a laser work" and therefore, "only dielectric walls would be suitable for a 10 micron

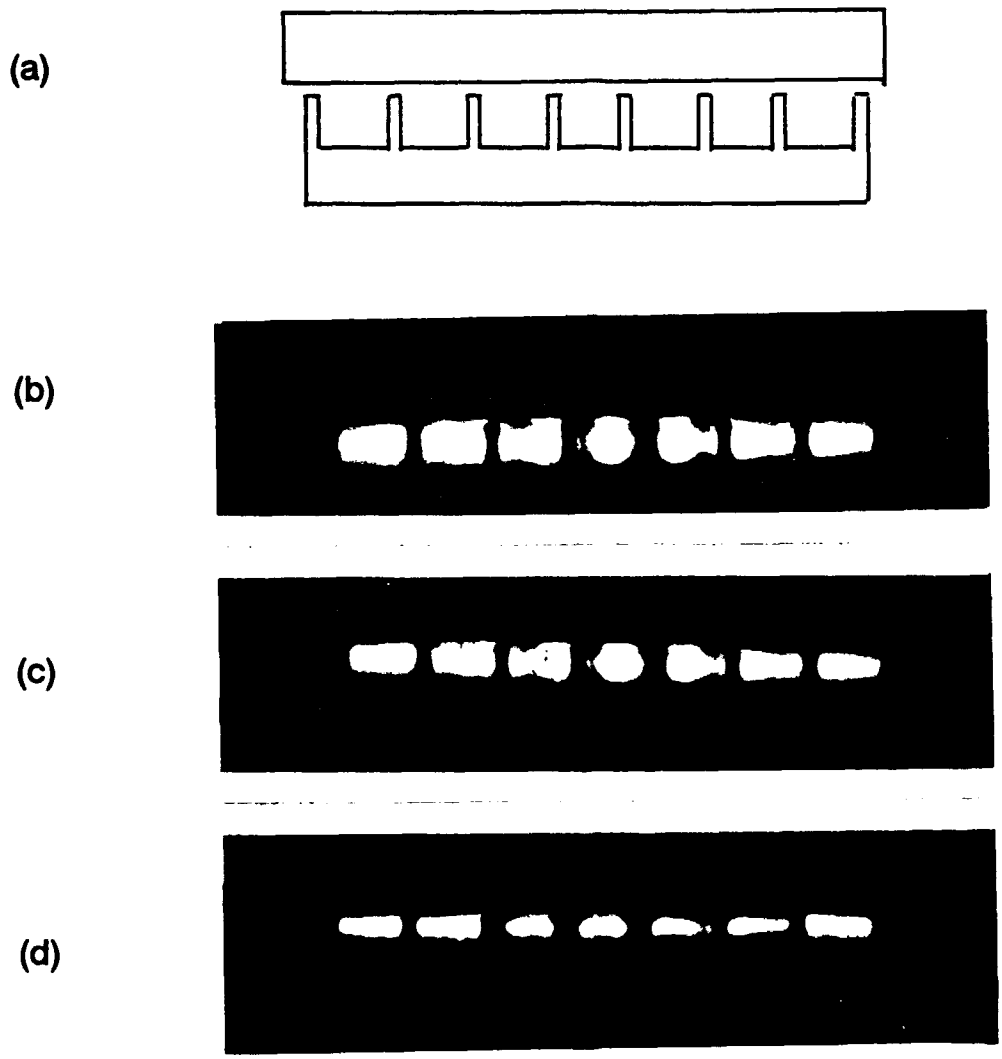

Fig.1 End view of 7-channel anodized aluminum test section at three different operating pressures: (b) 10.7 torr, (c) 18.1 torr, (d) 32.4 torr. Schematic view shown in (a).

waveguide laser." This was implicit in the paper by Abrams and Bridges[2], who evaluated the waveguide losses for SiO_2, Al_2O_3, and BeO waveguides as a function of wavelength using the known optical constants for those materials and the theory of Marcatili and Schmeltzer[3]. It is also implied in the paper by Laakmann and Steier[4] for r-f excited lasers, which considered four ceramic walls, or two ceramic and two metal walls; the case of four metal walls was not treated. Of course, it also true that at that time it seemed that no one had an idea how to excite a discharge in a structure with four metal walls with d-c or r-f! (Although we were not aware of it in 1988, Willets and Hartwright[5] had tackled the problem in 1978 and made a longitudinal d-c discharge waveguide CO_2 laser with four anodized aluminum walls, where the anodization (Al_2O_3) served as a d-c standoff as well as the optical guiding surface. Professor Denis Hall brought this reference to our attention in late 1989, after we were already doing our own experiments. Still later, Synrad Corp. advertised a four metal wall r-f excited laser, although the walls are not waveguiding[6].)

Following the "common wisdom", we investigated the optical properties of coated metal waveguides. A complete electromagnetic theoretical treatment had been given by Miyagi, et al[7-9], but this theory is rather complicated. Instead, we used a simple ray optics method (see, for example Yariv and Yeh[10]) that allows the calculation of losses in the case of a thin coating of lossy or low-loss dielectric on a metal surface. The relative propagation losses for coatings of Al_2O_3, SiO_2, and Ge on aluminum waveguides are shown in Fig. 2 for TE modes (electric field parallel to the surface) and in Fig. 4 for the TM modes (electric field normal to the surface). Figure 3 shows the relative TE-mode loss for thicker Al_2O_3 coatings. The relative loss parameter -ln(R) must be multiplied by a geometric factor depending on the cross sectional shape of the waveguide to determine the actual propagation loss constant, but correctly expresses the relative losses of identical guides made of different materials.

From these calculations we concluded the following:

(1) It is possible to use aluminum for two of the four walls and dielectric or dielectric coated metal for the other two walls. This was already suggested by Laakmann and Steier[4] and Adam and Kneubühl[11]. The mode of oscillation with select a polarization that will have its electric vector parallel to the metal walls.

(2) Coatings over aluminum of a lossy dielectric such as Al_2O_3 only a few microns thick will look just like an infinite thickness of the coating material. Thus dielectric walls in (1) can be metal underneath.

(3) Coatings over aluminum of a low or intermediate loss material such as Ge or SiO_2 can also be used to good advantage provided they are made the proper thickness (about 0.5 to 1 micron), and might be superior in waveguide loss to thick coatings of Al_2O_3. However, they are quite likely to be more difficult to apply and may be less durable in the discharge environment.

There remained the question of the waveguide losses due to scattering from imperfections in the surface, the "surface finish" required. Mr. Hart stated that UTOS used the Al_2O_3 parts "as ground" without further polishing, but did not have a quantitative value for the surface roughness. We had sent some aluminum pieces out for "thick anodizing" and then evaluated the results with a scanning electron microscope. The actual Al_2O_3 layer appeared to be about 5 microns thick, but the machined surface of the aluminum was significantly rougher than that, so we concluded that better machining or even additional polishing would be required to obtain low waveguide losses. We undertook a series of measurements in the final year of the program, and these are described in that section of this report. However, we determined empirically even before those measurements were made that we could successfully replace the Al_2O_3 ground waveguide arrays with machined aluminum arrays.

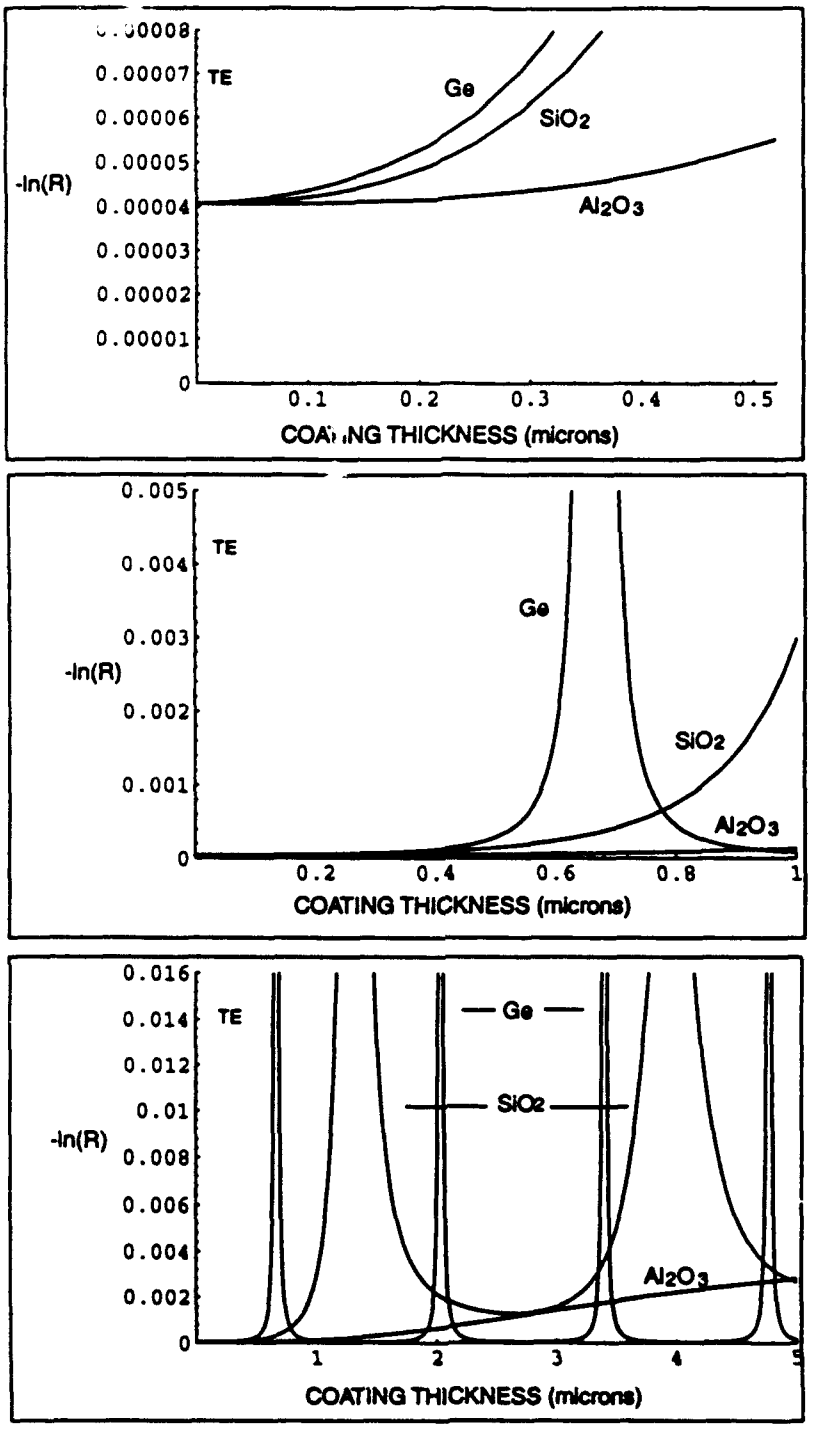

Fig. 2 Values of -ln(R) for Al_2O_3, Ge, and SiO_2 coating on aluminum as a function of coating thickness for TE modes and for various ranges: (a) 0 to 0.5 microns; (b) 0 to 1 microns; (c) 0 to 5 microns.

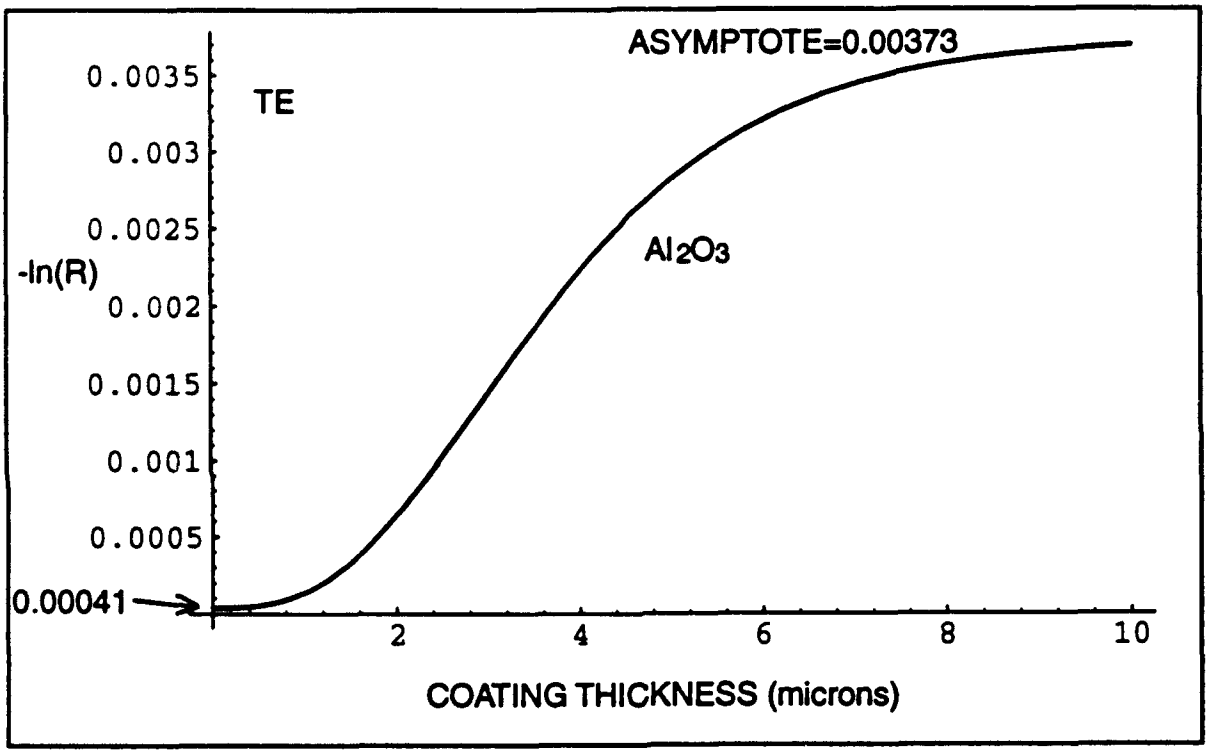

Fig. 3 Value of -ln(R) as a function of thickness for an Al_2O_3 coating on aluminum for TE modes.

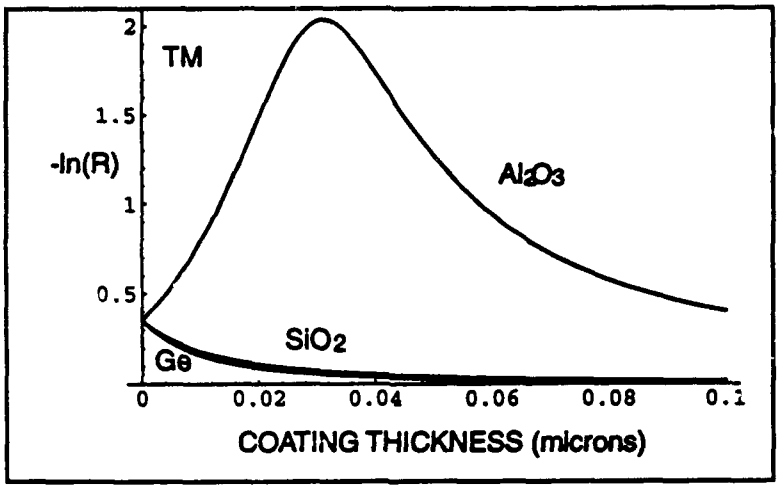

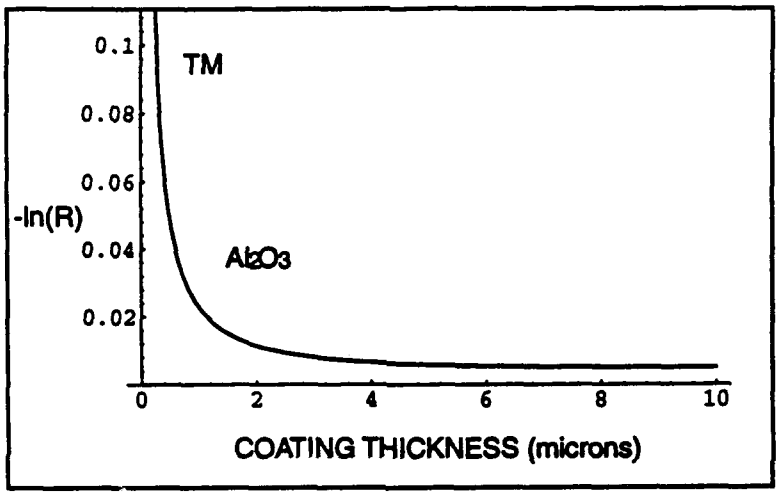

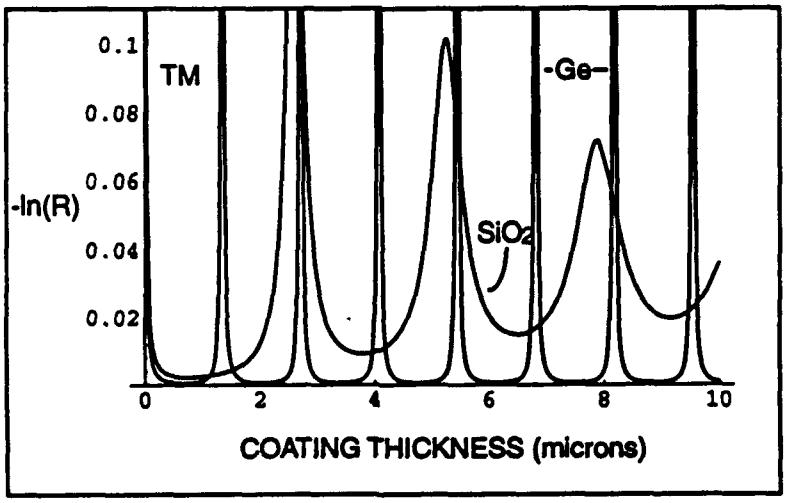

Fig. 4 Values of -ln(R) for Al_2O_3, Ge and SiO_2 coatings on aluminum as a function of coating thickness for TM modes and various ranges: (a) 0 to 0.1 microns, (b) Al_2O_3 0 to 10 microns, (c) Ge and SiO_2 0 to 10 microns.

C. LASER TEST BED

At the outset of the program we elected to make a "test bed laser" in which the laser active region could be easily interchanged without disturbing the mirror alignment, so that waveguide arrays could be checked one against the other with the minimum of modifications. This proved to be a wise decision, and the test bed laser has allowed us to try new arrangements very quickly.

The vacuum box of the test bed laser also serves as the optical bench for the laser mirrors, and thus required more structural strength than it would just to withstand one atmosphere pressure. The inside dimensions to the box are 6" x 6" x 18" and the wall thickness is 3/4". The box was fabricated by MDC Corp. of stainless steel, with welded-in vacuum flange fittings as shown in Fig. 5a. A photograph of the box with mirror adjustment micrometers installed is shown in Fig 5b. The aluminum box on top houses the r-f matching network. The water cooled waveguide clamp is supported off the top cover, and is shown in Fig 6a. A two-channel waveguide is fixed in the clamp in this particular picture. An exploded view of the clamp structure is shown in Fig. 6b. Figure 7a shows a sketch of the water channels in the clamp structure, and Fig 7b is a photograph of end, showing a two-channel aluminum waveguide in the clamp. To change waveguide arrays, this water-cooled clamp is loosened and a new waveguide "sandwich" is inserted and the matching adjusted. The procedure takes about 10 minutes.

The waveguide "sandwich" and clamp structure looks electrically like about 600 pF of capacitance, which is resonated at 146 MHz with several shunt inductors added in parallel, as shown schematically in Fig. 7a. In actual practice, these inductors are really a pieces of copper shim stock connected between the waveguide pieces over most of the length of the waveguide. Connection to the "hot" side of the clamp is made through a vacuum feedthrough in the top of the box, and into a shielded impedance matching network. Considerable trial and error ensued in arriving at a successful arrangement. Plasma breakdown in the feedthrough and insufficient shielding (resulting in upset of most of the lab's measuring instruments!) were only two problems that had to be overcome. The impedance matching network was not a simple linear design problem, since it had to satisfy two requirements: It had to match the 50 ohm output of the power source into the resonant structure to create a high voltage that strike the plasma, then provide a proper match after the plasma formed. This also required a trial-and-error approach.

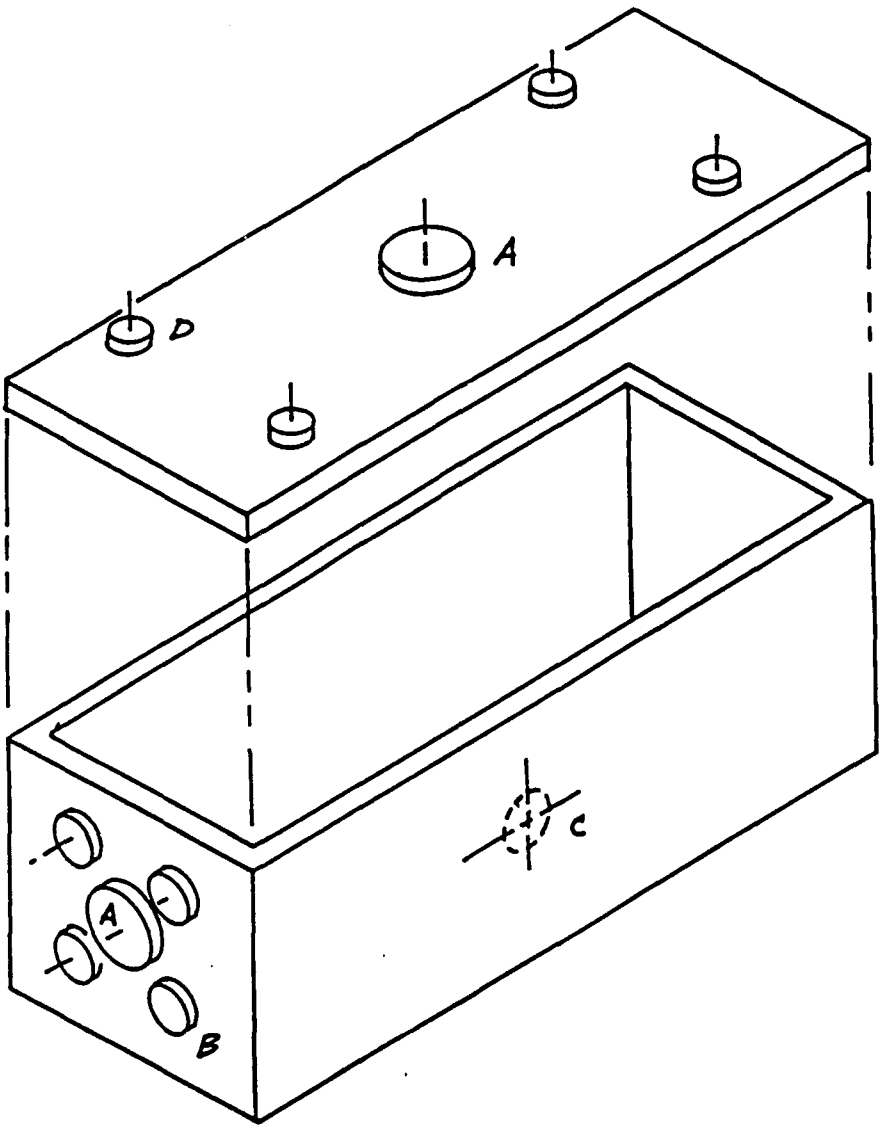

Fig. 5a Sketch of the testbed laser vacuum box assembly. (Repeated from the first annual report, Ref. 1) Inside dimensions of the welded stainless steel vacuum box are 6" × 6" × 18". Fittings welded on A = 2 3/4" Del-seal flange; B = Del-seal miniflange; C = Bolt circle for kwikflange bulkhead fitting K075-BC; D=1/4" pipe coupling welded on, with additional 1/4" pipe thread tapped from below.

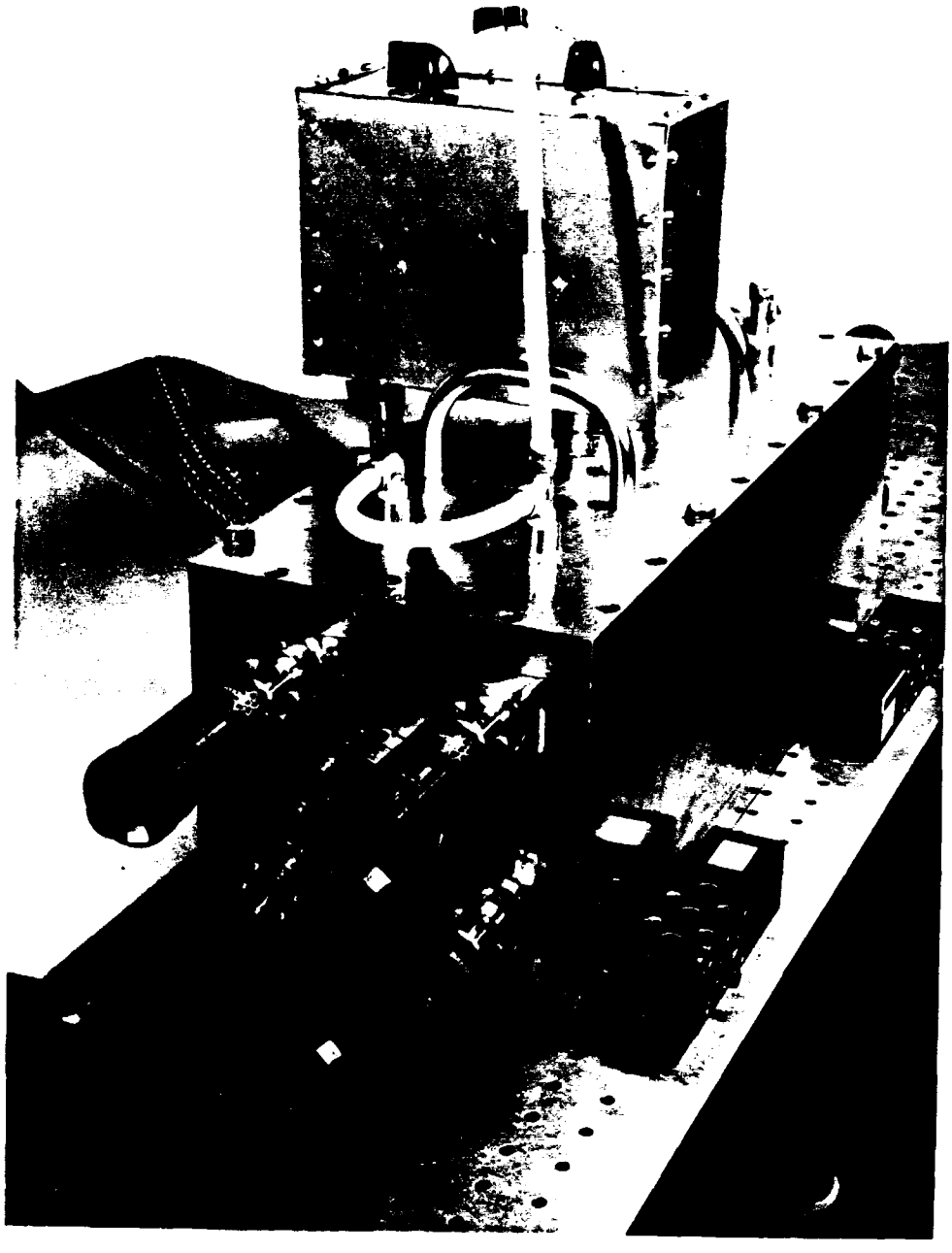

Fig. 5b Photograph of the test bed laser. The aluminum box on top of the vacuum box contains the r-f matching network.

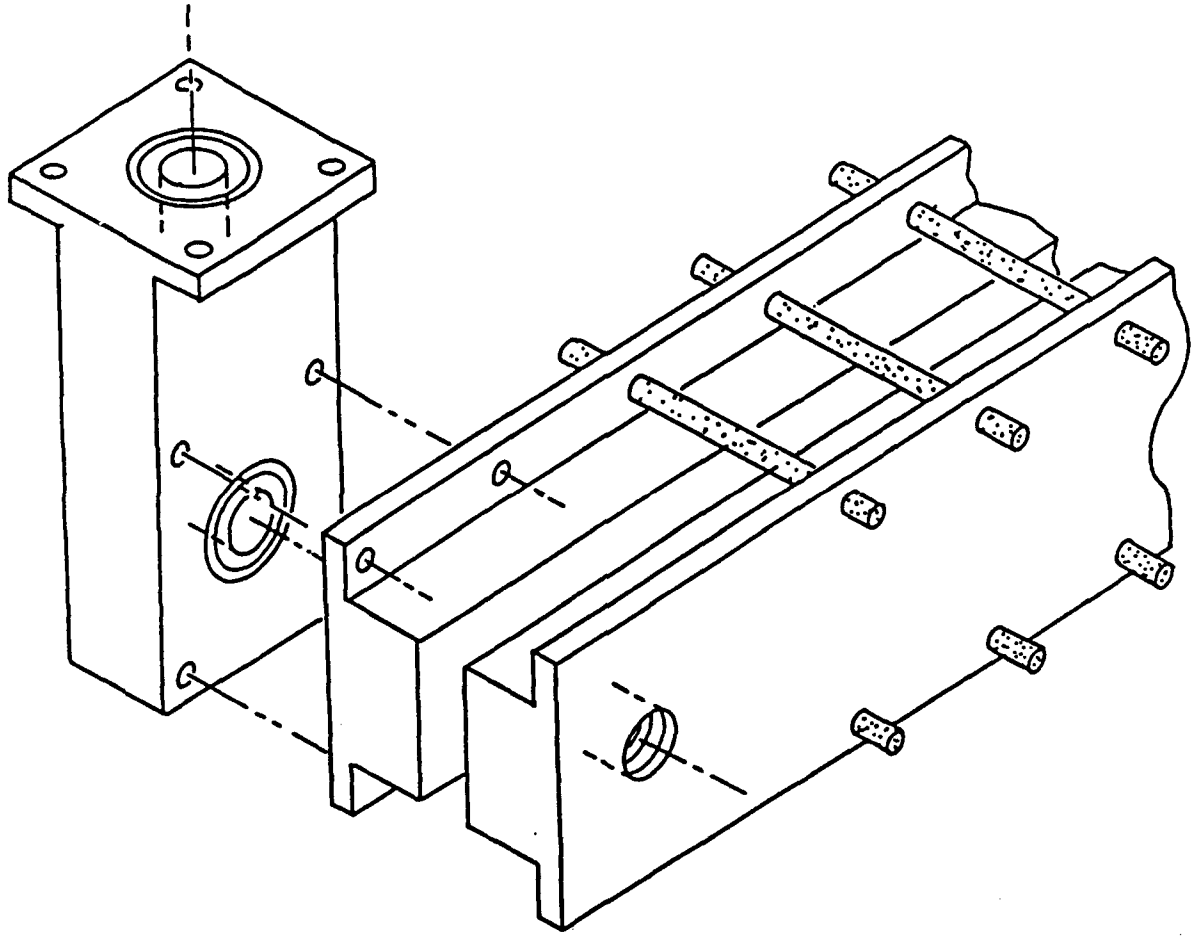

Fig. 6a Exploded-view sketch of water-cooled electrode holder assembly (Repeated from first annual report Ref. 1).

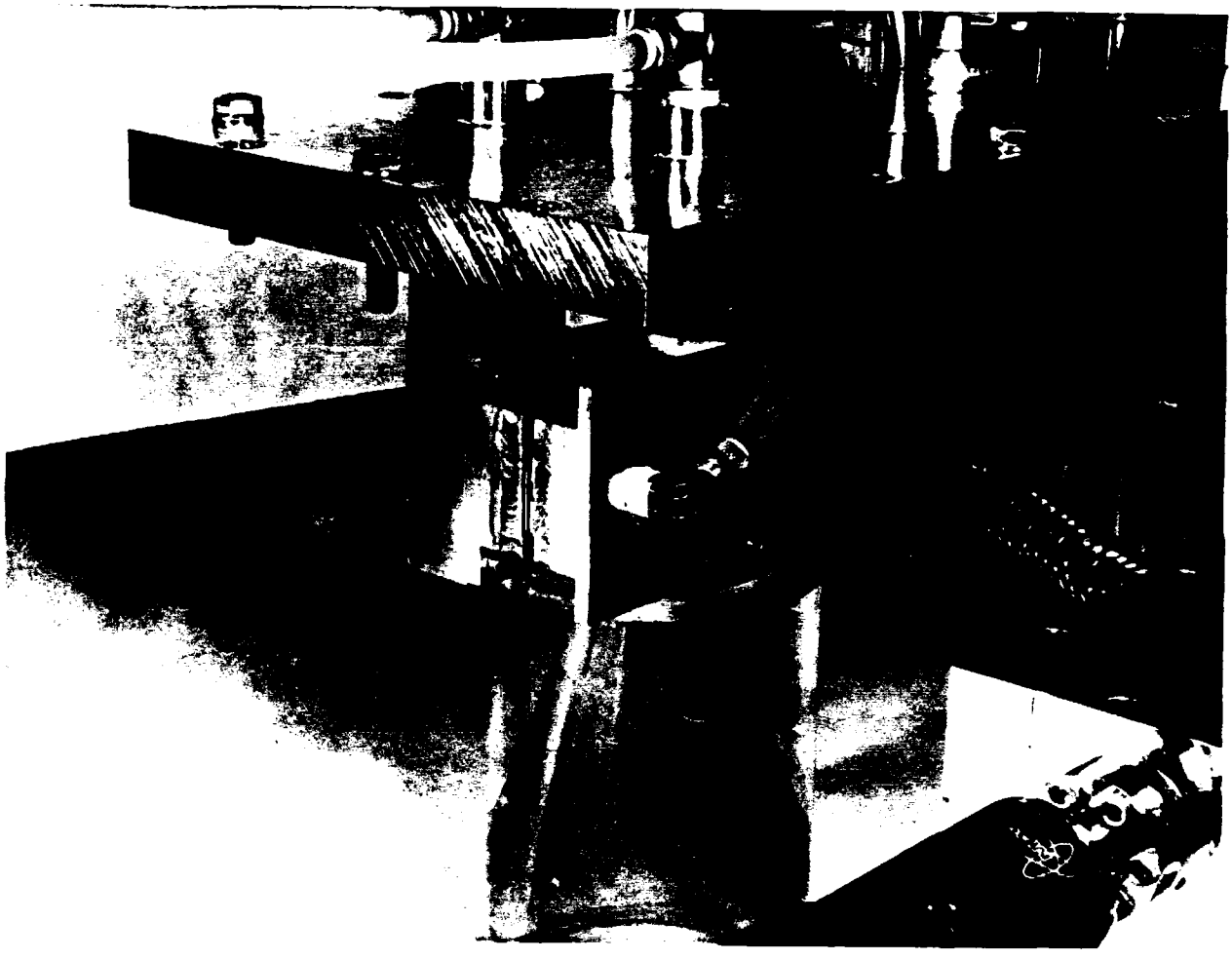

Fig. 6b Photograph of water-cooled electrode holder assembly affixed to the cover of the vacuum box.

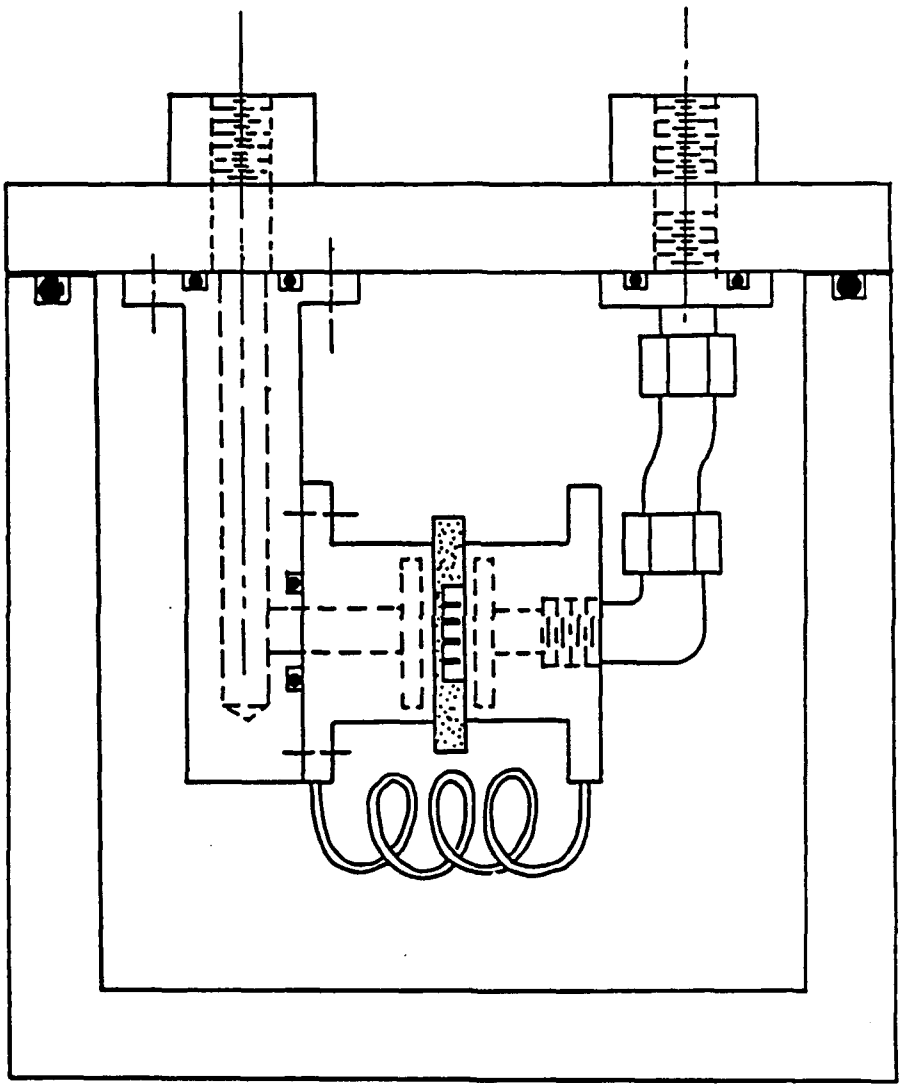

Fig. 7a Sketch of the water-cooled electrode assembly with the water channels shown in dashed lines (Repeated from first annual report Ref.1)

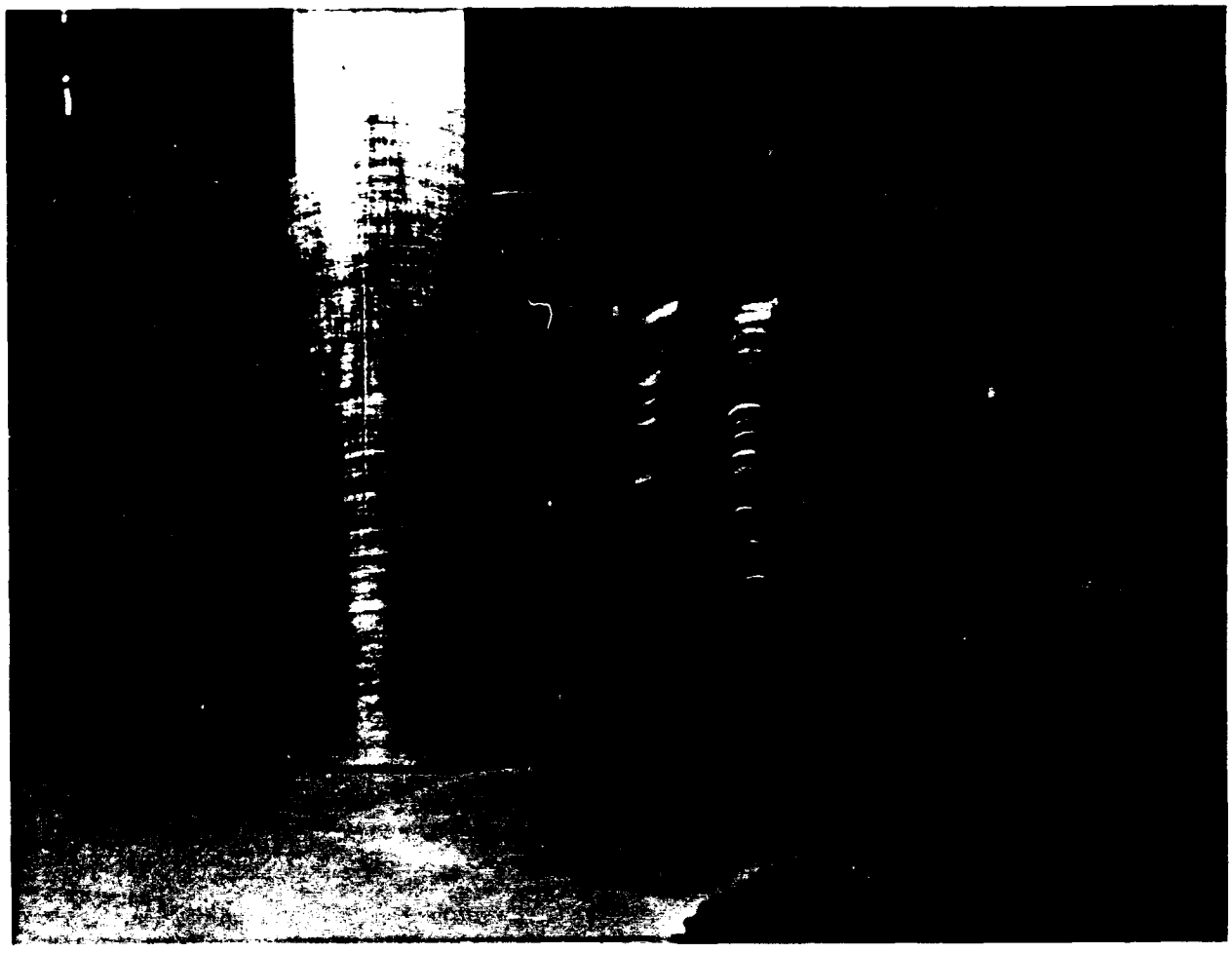

Fig. 7b Photograph of the end of the water-cooled electrode holder showing the heliarc joint on the periphery. The two-channel waveguide shown in this particular photograph is our experimental "bare aluminum" version.

The network shown in Fig. 8a was successfully implemented and was used for initial experiments. However, there were continued problems with the air dielectric variable capacitors used when operated at high input powers, of the order of a kilowatt. A second circuit was developed that used vacuum variable capacitors as shown in Fig. 8b to eliminate this problem.

Two sets of power sources were used for the experiments. The initial experiments used an ICOM IC-28H amateur radio transceiver (45 Watt output) driving an R-F Concepts model 2-417 solid state power amplifier (175 Watt output.) For higher power experiments, a Kenwood TS-711 amateur radio transceiver (100 Watt output) driving a Henry Radio 3002 vacuum tube linear amplifier (1.5 kw output) was used. This latter combination had the added advantage of a smoothly variable power control. A Bird Thruline Model 43 directional power meter was used for input and reflected power measurements.

D. TEST BED CALIBRATION AND PARAMETRIC PERFORMANCE

In order to assure ourselves that our test bed laser was operating correctly, we undertook a series of measurements using ceramic bore samples that were loaned to us by the UTOS group. The particular channel arrays are shown in Fig. 9. Both coupled and uncoupled two-channel arrays were evaluated. The gas mixture used was chosen to be as close to that used at UTOS: N_2:CO_2:-He:Xe=1:1:6:0.25. The mirror output coupling was the same, 10% transmission. The power source frequency was 146.56 MHz, essentially the same. The highest single-point power measurement with our test bed laser using the coupled array was 41 Watt output at 432 Watt input at a pressure of 113 torr, for an efficiency of 9.4%. The output power was measured with a Coherent 201 power meter. The highest single-point efficiency with the same ceramic piece reported by UTOS was 47 Watt output at 425 Watt input for an efficiency of 11%. We suspect the small difference may lie in the poorer cooling our "pressure-clamp" structure provided; the UTOS structure was somewhat superior in thermal design. And our mirrors were obtained from a different source than the UTOS mirrors. Nevertheless, we were satisfied that we were close enough to the UTOS results for our purposes.

Figure 10 shows the power output versus r-f power input for the testbed laser with the coupled two-channel guide, with fill pressure as a parameter. Figure 11 shows the output power as a function of gas fill pressure with the r-f drive power adjusted to its optimum value.

(a) First network. L1 and L2: 4 1/2 turns, 5mm OD copper tubing, 22mm diameter, 34mm long, 50 mH; C1 and C2: variable air capacitors, 10 to 25 pF air value (3mm plate spacing).

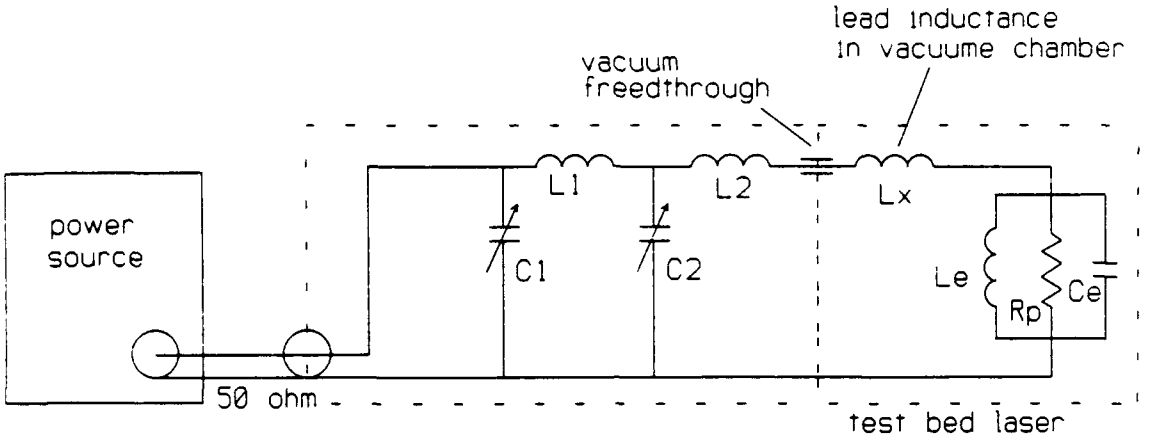

(b) Improved network for high power operation. L1 is the same as before. C1 and C2 are Jennings vacuum capacitors, 5 to 25 pF.

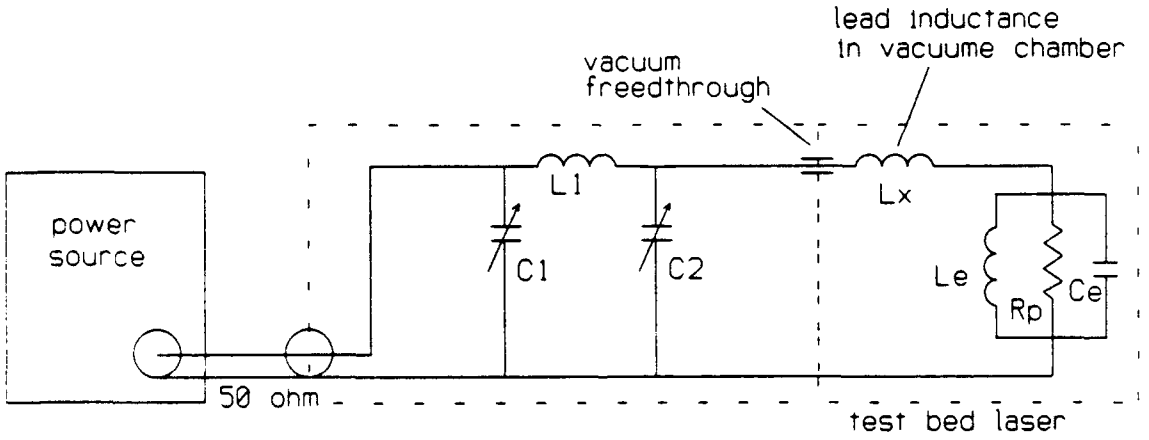

Fig. 8 Schematic diagrams of r-f impedance matching networks used in these experiments: (a) during the initial phase and (b) improved for high power operation.

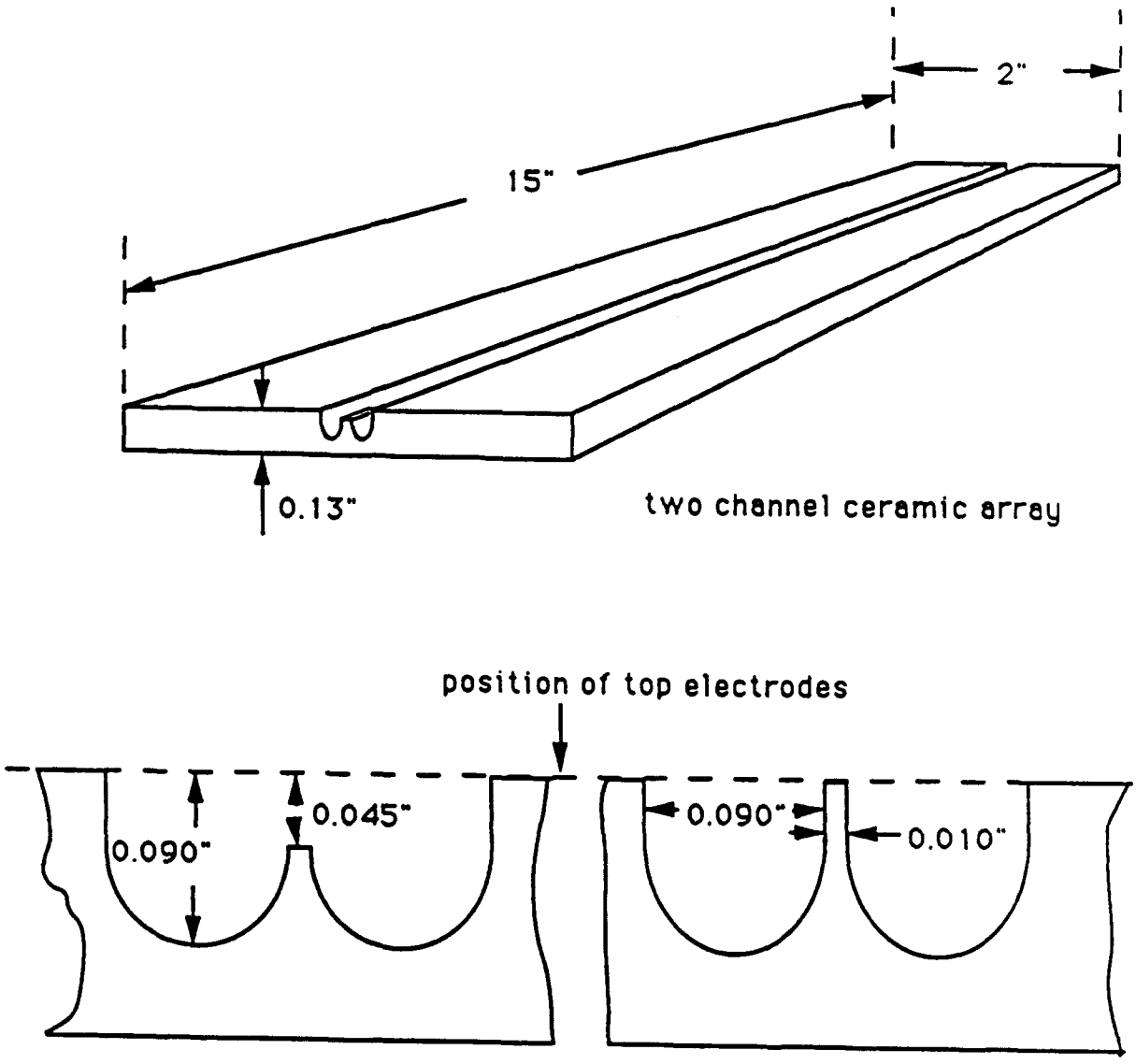

Fig. 9 Sketch of UTRC ceramic two-channel waveguide showing dimensions. Details of the coupled and uncoupled arrays are shown in the blow-ups a) and b). They are different only by the gap.

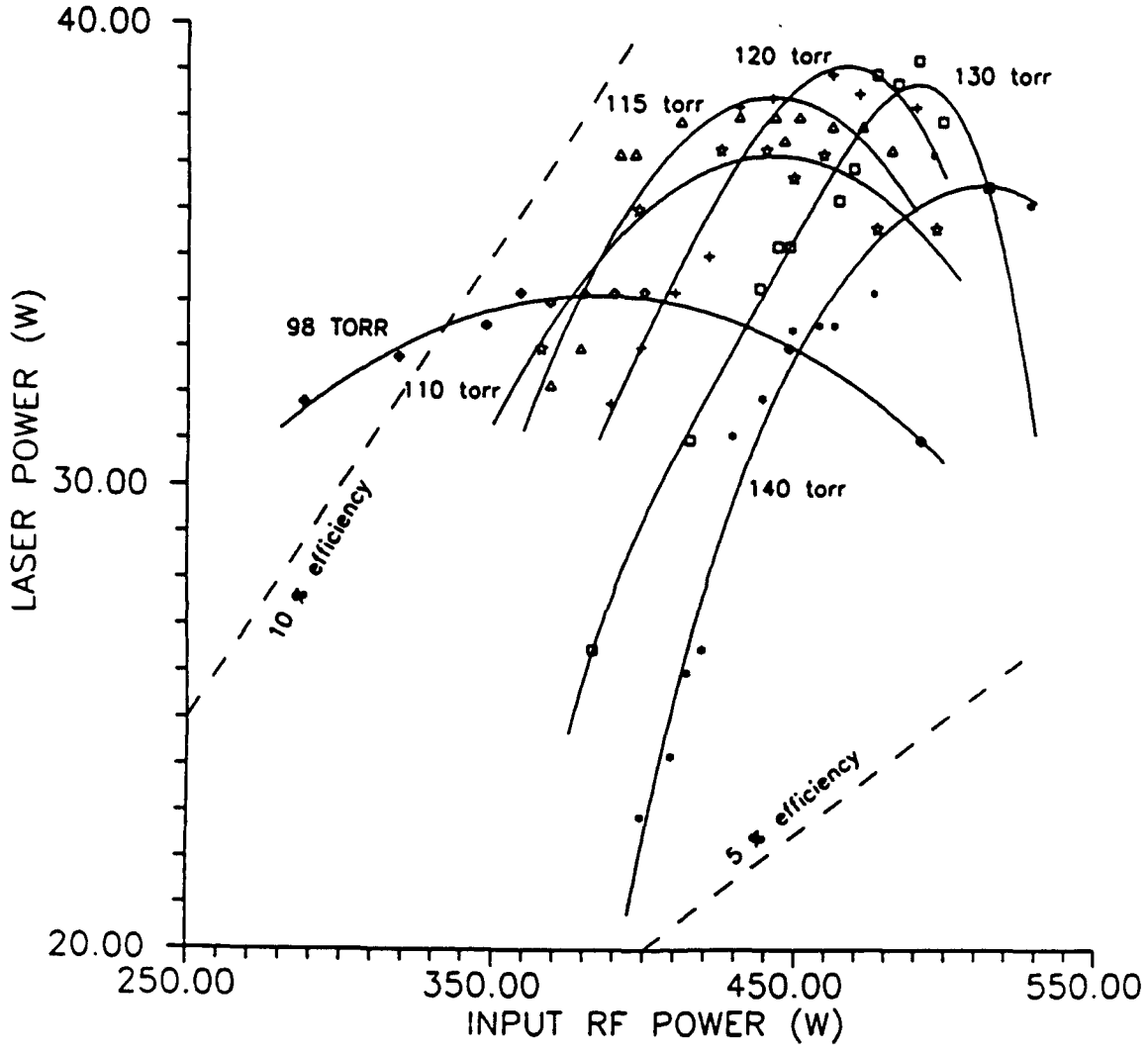

Fig. 10 Tested laser power output v.s. r-f drive power at 146 Mhz for the two channel guide shown in Fig. 9 with pressure as a parameter. Lines of constant efficiency are also shown at 5% and 10%.

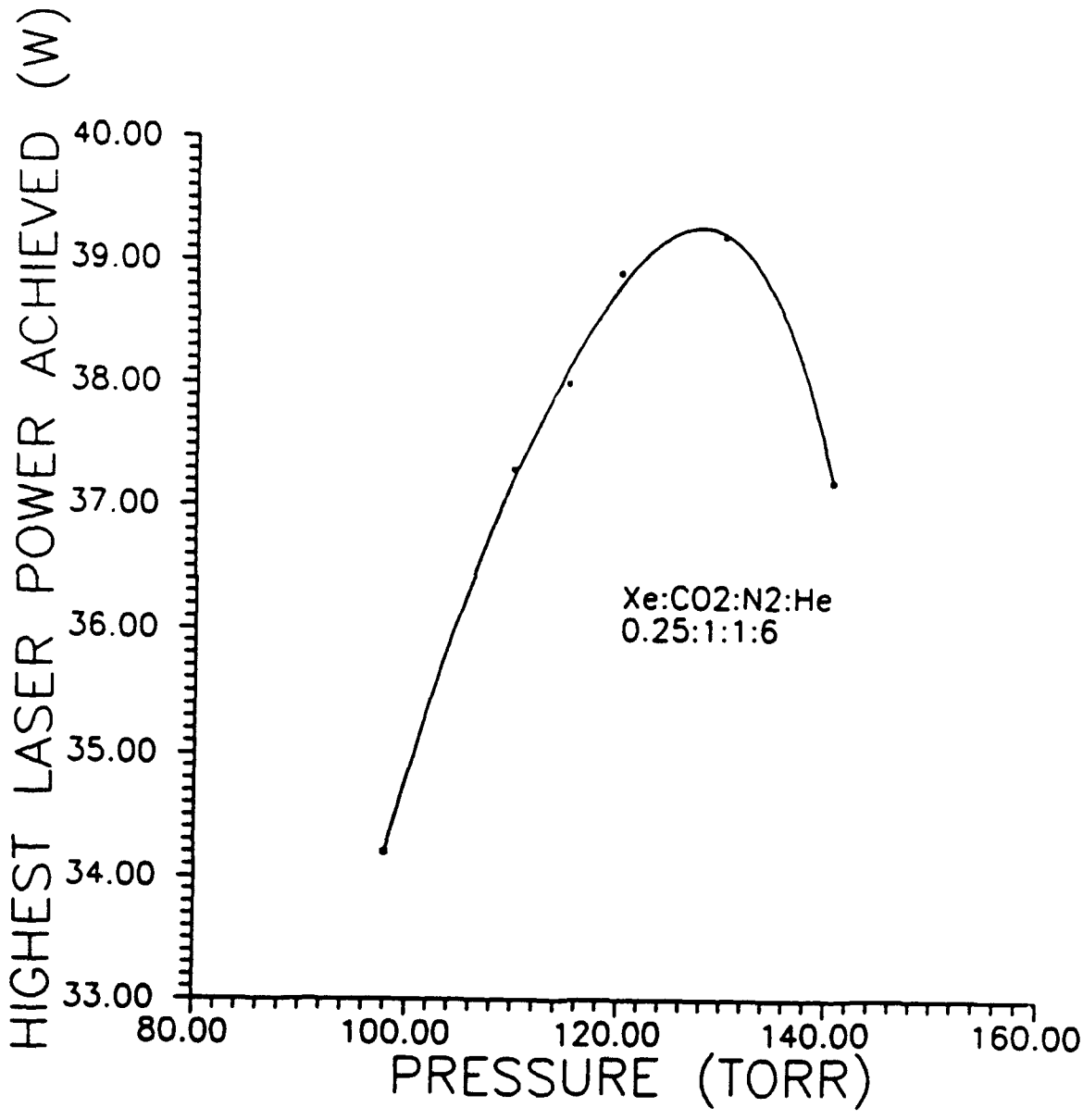

Fig. 11 Data of Fig.10 re-plotted to show maximum output v.s. gas pressure with the r-f drive power optimized at each pressure.

E. MODE COUPLING EXPERIMENTS

The diagnostic setup for these experiments is shown in Fig. 12. A silver-on-copper diffraction grating was used to split the laser output into two channels. An Optical Engineering model 16-A spectrometer was used to monitor the vibrational transition. A Boston Electronics model R004-0 fast HgCdTe photodetector was used with a Hewlett-Packard hp 8554B spectrum analyzer to detect beat notes. Near-field spatial mode patterns were monitored with Optical Engineering quenched fluorescence image plates inserted into the paths and photographed with a 35mm camera. A lens pair could be inserted ahead of the image plates to obtain the far field pattern as well. Total power was measured by inserting a Coherent 201 power meter into the laser output.

Figure 13 shows the typical behavior of the beat spectra and mode patterns for the coupled two-channel guide. In these patterns "0 Hz" is the large spike artifact at the left edge of the photograph, and the rightmost spike is leakage of the r-f power source at 146.505 Mhz, which was convenient as a frequency marker. The mode patterns are the corresponding far field coupled mode patterns. The beat spectra observed usually contained more than one component because the UTOS waveguide channels were a bit too large to select a single transverse mode each; thus both waveguides were multimode individually, so when they operated in an unlocked fashion, several components could be observed, rather than just one, and when locked, there would still be residual beats from the multiple modes. Although not mentioned in their reports, Mr. Hart confirmed verbally that they typically saw the same thing and attributed the complex spectrum to multimoding in each guide.

The two channel coupled guide illustrated in Fig. 9 could be operated stably in either the in-phase (symmetric) or the out-of-phase (antisymmetric) state for hours at a time. Figure 14 shows the spatial far-field patterns obtained with (a) inphase locking, (b) out-of-phase locking and (c) unlocked operation. Shifting between states required only a slight mirror adjustment. However, we noted that the out-of-phase state would persist over a wider range of mirror adjustment than the in-phase state. This is consistent with the picture, first suggested by the UTOS group[12], that the out-of-phase locked state has higher gain and is thus more stable because it has a zero in its field distribution just where the intervening wall introduces physical obscuration. This is illustrated in Fig. 15.

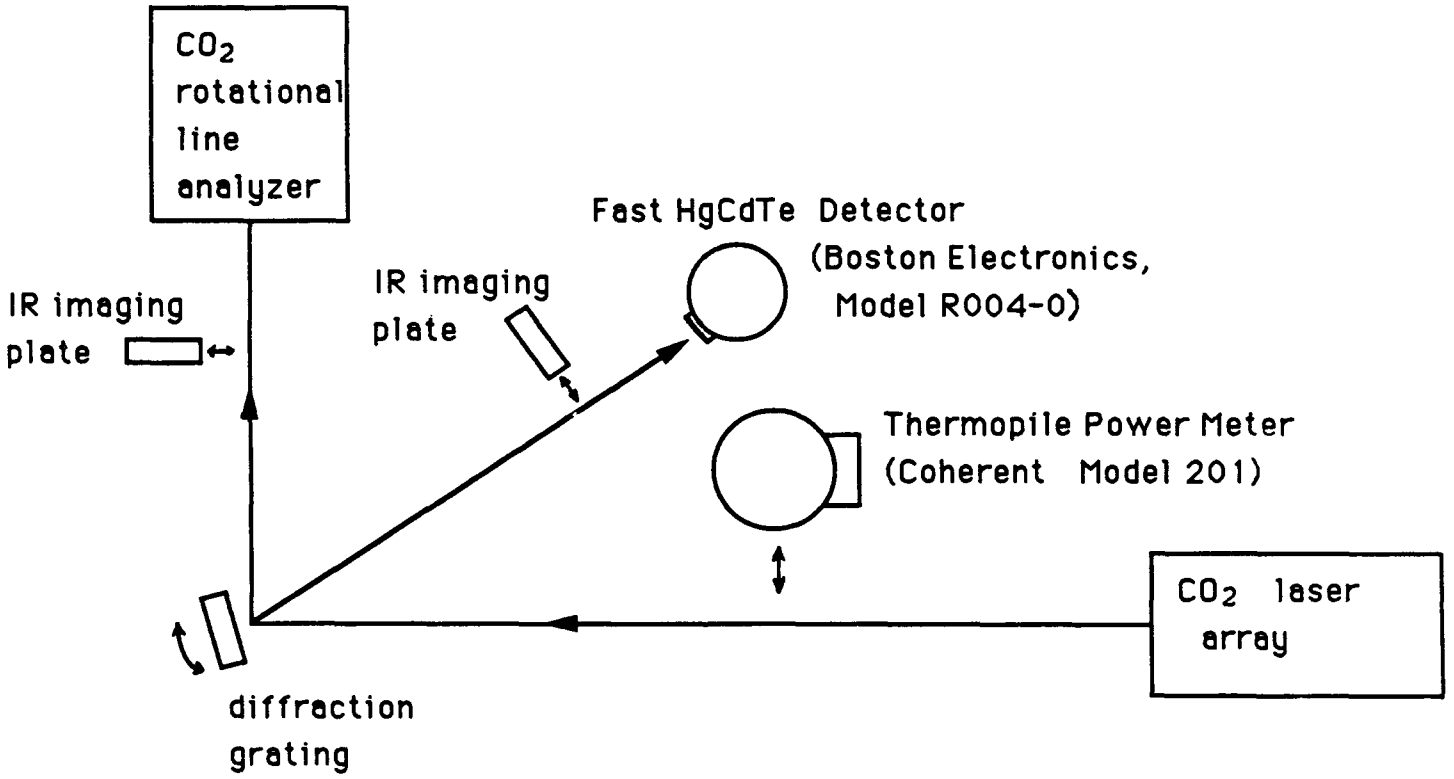

Fig. 12 Experimental arrangement for mode coupling measurements.

To confirm this picture, we ran a test with a small additional loss in the wall region, introduced by gluing a tiny glass chip to the dividing septum on one end of the guide, as shown in Fig. 16. Radiation is still to couple from one guide to the other over the remaining portion of the guide, so coupling and locked operation is still obtained. We were able to obtain good antisymmetric mode locking as indicated by the far field pattern and the lack of beats on the spectrum analyzer, but we were unable to obtain symmetric or in-phase locking.

As an experimental side observation, we note that multimode behavior of the basic channels produces a further complexity in the measurement process. The complex spectra shown in Fig. 13 were obtained with an attenuated sample of the entire transverse output beam incident on the photodetector. If various regions of the output beam were masked, the spectrum would change. For example, the antisymmetrically locked state produces a two-lobed far field pattern, as shown in Fig. 17. If the channels operate multimode each, there will still be some beat notes in the frequency spectrum, and these beat notes arise from modes with different spatial distributions. Thus, if the photodetector sampled only region a. in the figure, we would observe two beat notes at 19.5 and 17 MHz. If the photodetector were masked so that only region b were sampled, then the 19.5 MHz beat note would disappear, but the 17 MHz note would remain. Obviously, one of the mode distributions responsible for the 19.5 MHz beat has a null in its distribution at the center, likely the main antisymmetric-locked beam. Of course, if both channels are small enough to be single mode, then no beat notes should be observed under locked conditions.

Another result from our early mode studies was the observed variation of mode and power variation with angular mirror tilt and axial displacement. (In our mirror adjustment scheme, moving any one micrometer results in both tilt and axial displacement. We had hoped to add stepper motor drives to the micrometers and use computer control so that drives could be applied simultaneously to multiple micrometers that would correspond to pure tilt or pure displacement, but neither time nor funds allowed it.) Figure 18 shows the variation of a two-channel array with tilt angle, exhibiting the output power peaks, indicated by (*), where the far field patterns were also "simple"; and the output power minima, indicated by the shaded region, where the far field patterns were irregular and the power output unstable. We would expect the two channels to lock and unlock periodically as the optical cavity lengths and hence the resonant frequencies for the two channels are changed differentially

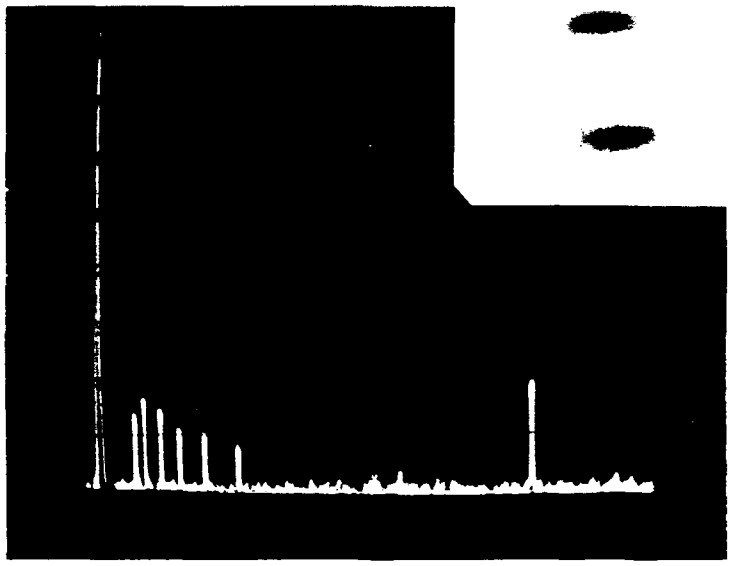

Fig. 13 Typical beat spectra for the two-channel guides.

a. A multimode structure.

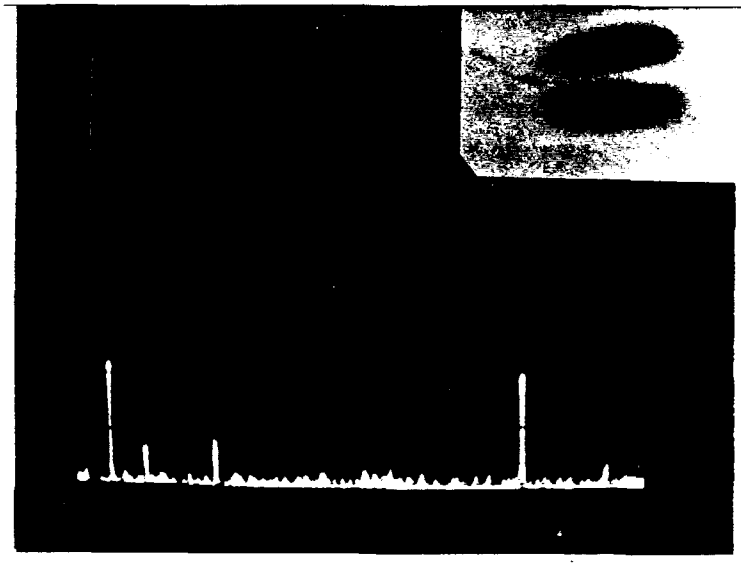

b. Relatively simple coupled mode structure, but still multimode.

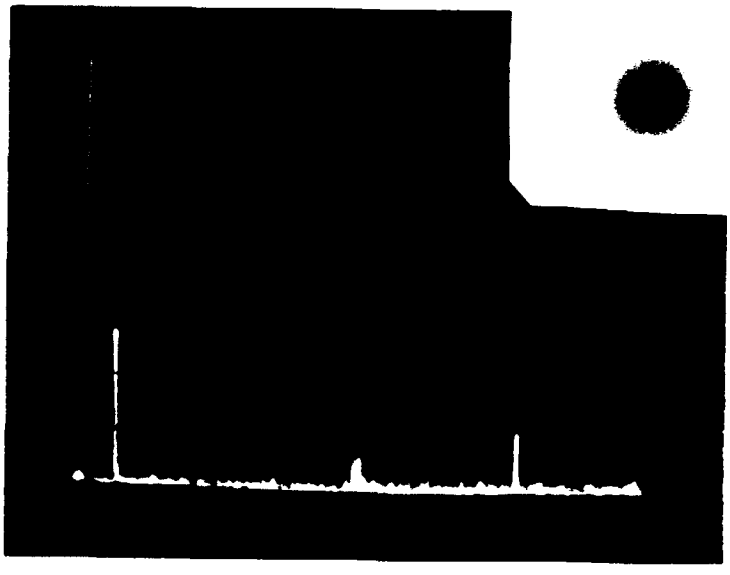

c. Mode from the uncoupled array. Only a single lobe is seen.

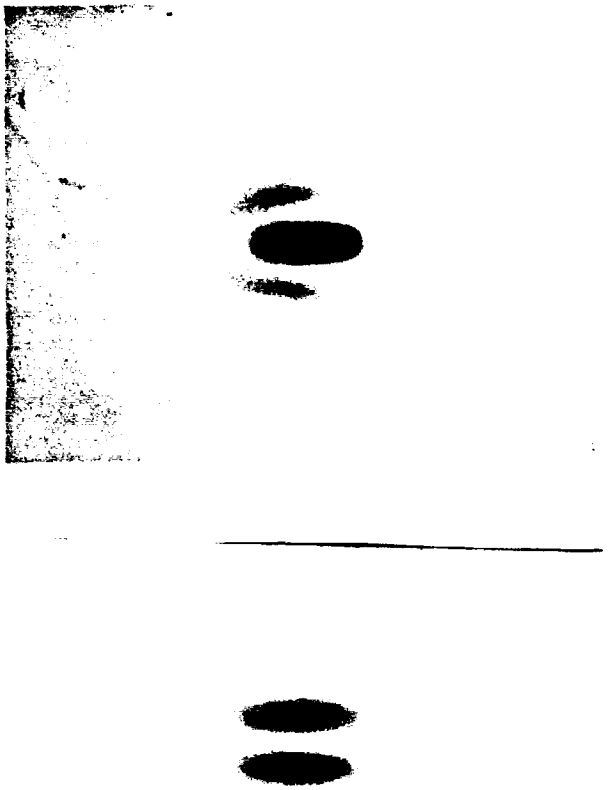

Fig. 14 Far-field spatial mode patterns for different locking conditions: a. Phase-locked in the symmetric mode, b. Phase-locked in the antisymmetric mode, c. Not phase locked.

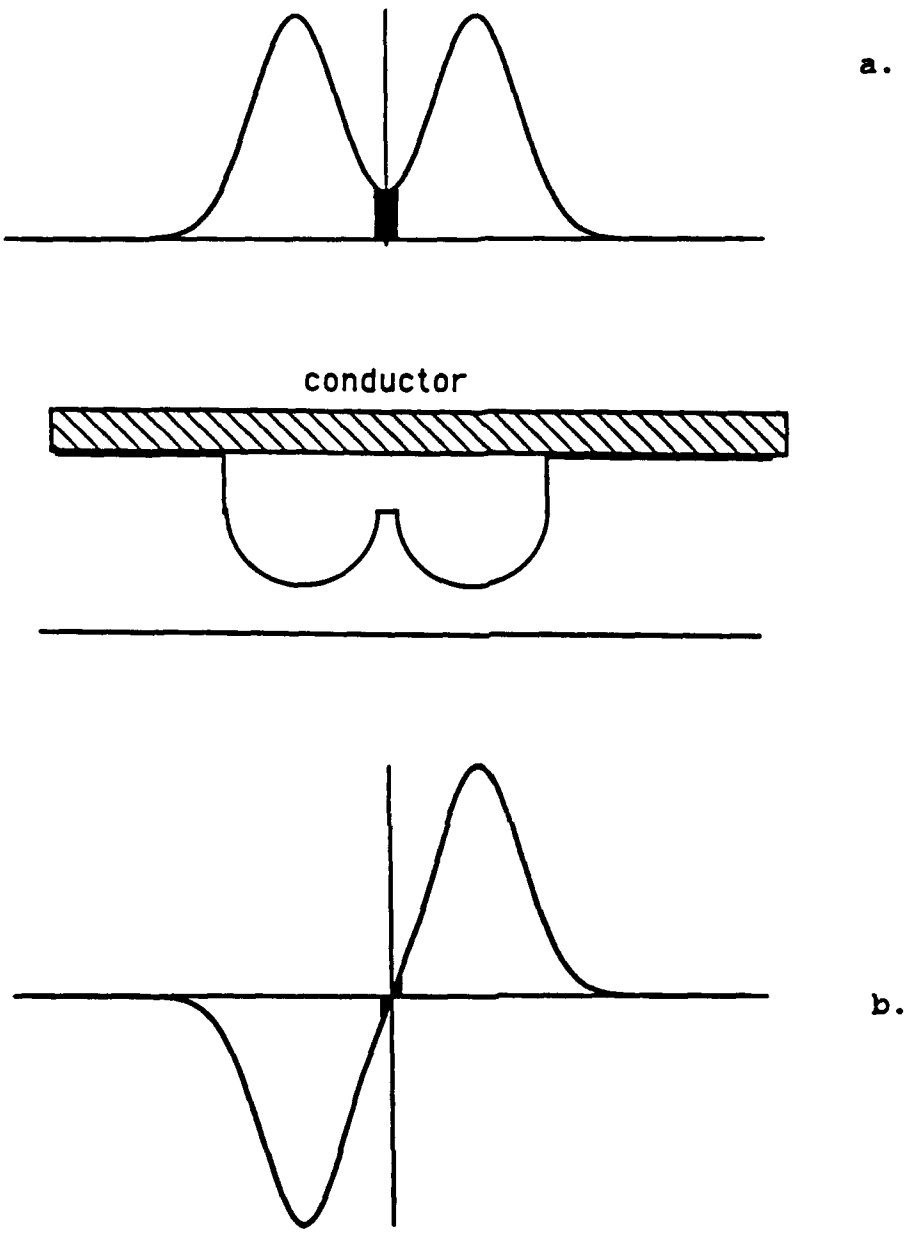

Fig. 15 Schematic representation of the effects of optical loss introduced by the separating wall on: a. The symmetric mode and b. the antisymmetric mode. The shaded areas indicate the mode overlap with the high loss introduced by the channel wall.

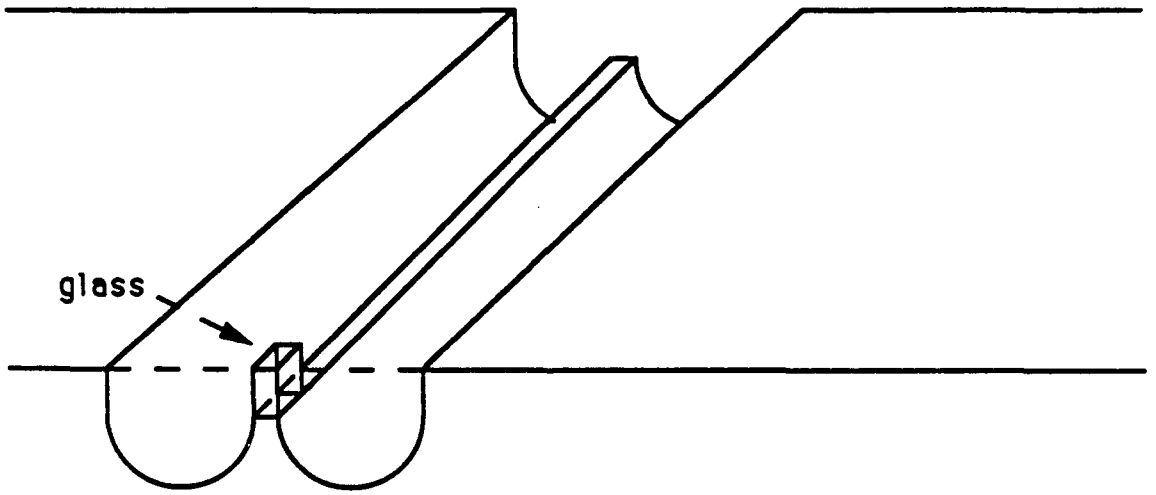

Fig. 16 Sketch of the end region of the coupled two-channel UTRC guide with a small glass tab added as a higher order mode suppressor.

by the "tilt". However, Fig. 18 is for the two uncoupled channels! For these, we would expect only a smooth change in beat note, but no change in output power or in mode pattern (since the two channels would be operating on different frequencies, and thus be incoherently added.) And the coupled channels exhibit identical behavior. We do not have an explanation for this behavior.

F. PARALLEL-PLATE WAVEGUIDE EXPERIMENTS

We originally conceived the parallel plate waveguide experiments as a vehicle for evaluating the surface roughness and dielectric coating effects in determining the waveguide propagation losses. However, it became readily apparent that parallel-plate waveguides had a lot to offer in their own right. We began the experiments with simple machined-surface aluminum plates, 20 mm wide and 370 mm long, spaced 1.8 mm apart. (This is the same length and approximate height as the two channel array, but is substantially wider: 20 mm compared to about 5 mm). We initially obtained a maximum output of 29.3 Watt at 500 Watt input at 36.6 torr pressure, for an efficiency of 5.9% without xenon in the gas. By adding xenon, we were able to increase the efficiency to 8.6% with 21.5 Watt output at 250 Watt input and 44.6 torr total pressure. Later with the addition of the Henry Radio Model 3002A linear amplifier, we were able to obtain a maximum output power of 75 watt at 975 watt input at 110 torr pressure for an efficiency of 7.6% without Xe in the gas. With 3% of Xe in the gas, we obtained a maximum output power of 86 watt at 875 watt input at 120 torr total pressure for an efficiency of 9.8%.

These numbers, while not as good as those with the coupled channel arrays, were good enough to cause use to consider what we might do with the parallel plate geometry.

The mode structure out of this laser was also very interesting. With flat mirrors, it looked very much like a single, high order gaussian mode in the 20 mm direction and a single mode in the "waveguiding" or 1.8 mm dimension. The discharge was well behaved, filling the space uniformly without "filamenting", so the almost ideal behavior of the mode shouldn't have surprised us.

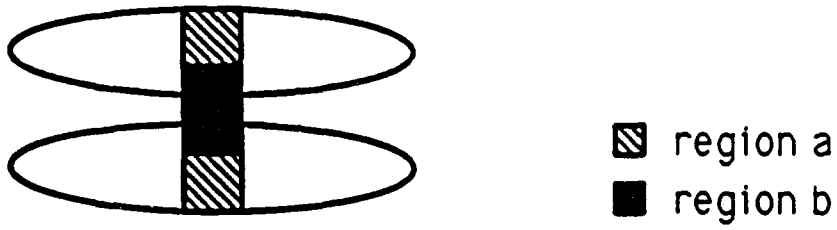

Fig. 17 Schematic drawing of a antisymmetrically locked far field pattern showing the region scanned by the fast detector (shaded) and the regions of two-beat spectra (a) and the region of one-beat spectra (b).

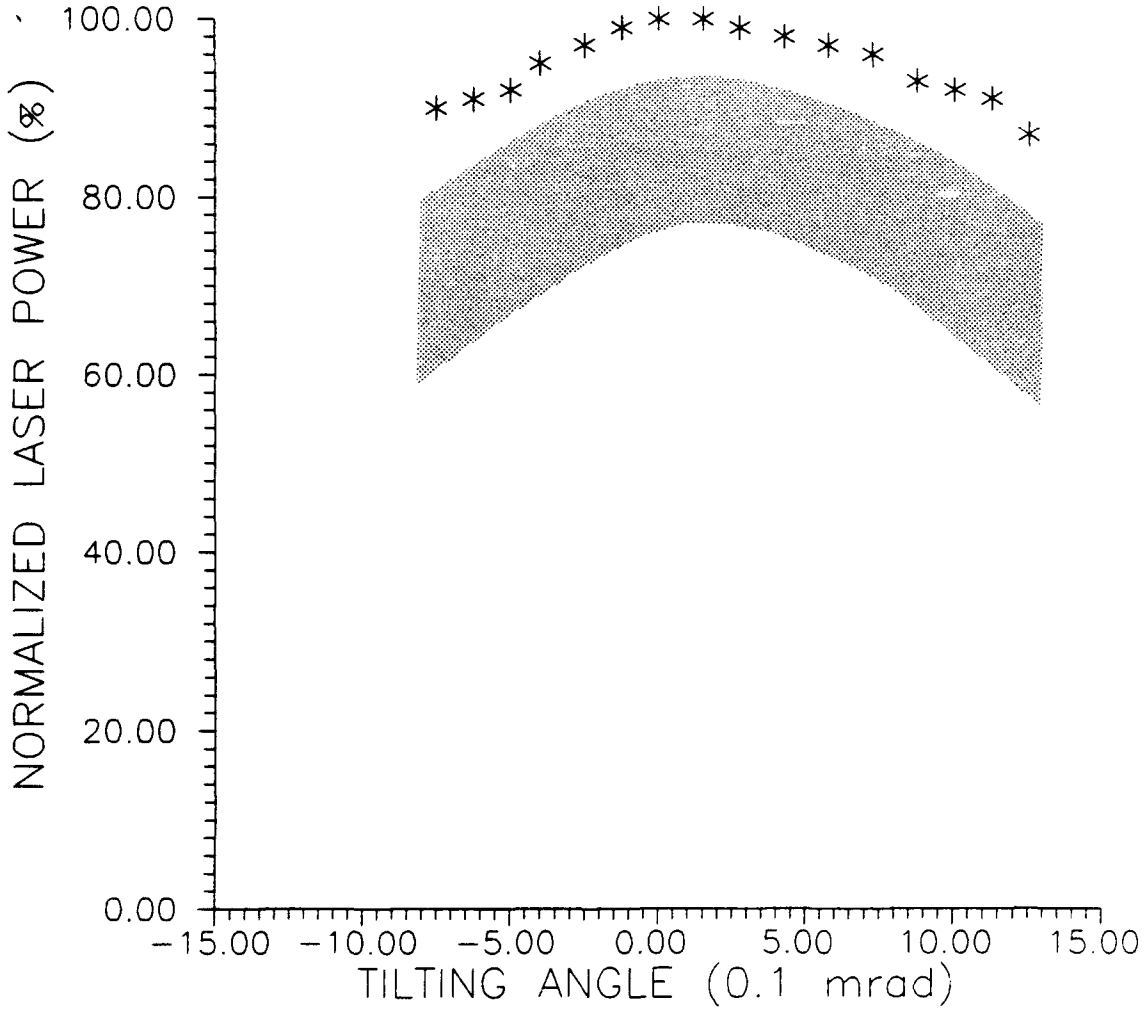

Fig. 18 Variation of the UTRC uncoupled two-channel array output power with mirror tilt (and displacement) showing periodic behavior. The stars indicate the peaks of output power and "clean" far field mode patterns. The shaded area indicates where the minima between peaks fall.

To see if this situation was as ideal as it appeared, we replaced the high reflectance mirror with a polished brass shim mirror that could be deformed into a cylindrical shape in the waveguide width dimension while the laser was operated (with the spare micrometer port.) While the output power was greatly reduced by using this uncoated, lossy mirror (typically 2 Watt with 280 Watt input), we could demonstrate a sequence of ideal "Gaussian - waveguide" modes; that is, modes that were free-space Gaussian in the width direction and cosine in the height (1.8 mm) direction. This sequence is shown in Fig. 18 a-d. Additionally, higher order waveguide modes could be produced by tilting the mirror in the guiding direction, as shown in Figs. 18 e-f, and more complex patterns could be obtained by tilting the mirror in both directions, Figs. 18 g-i. These results encouraged us to believe that it would be relatively easy to obtain a high quality, single mode output from such a slab laser by the simple expedient of using a cylindrical mirror unstable resonator. Thus our set of experiments to look at waveguide surface effects took on a whole new aspect of an improved, simplified laser that might result from two simple metal plates.

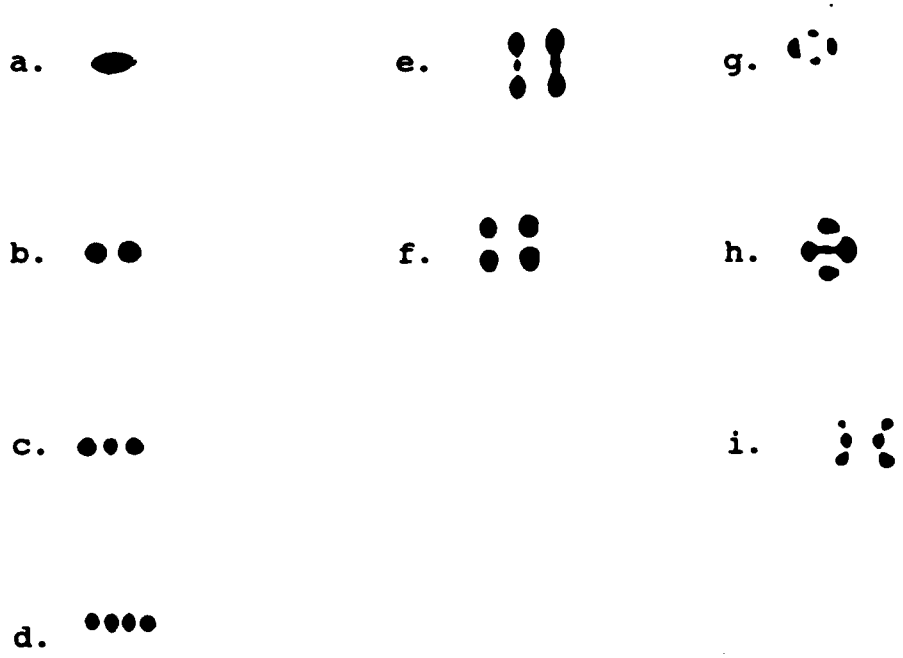

Fig. 19 Mode patterns for a parallel-plate laser. a-d were obtained by changing the curvature of a cylindrical mirror on one of the lasers. e and f were obtained by tilting the mirror perpendicular to the plates. g through i were obtained by tilting the mirror in box x and y directions.

PROGRESS IN THE THIRD YEAR

A. CONTINUATION OF THE PARALLEL PLATE MEASUREMENTS.

1. Comparison of Experimental Results for Different Surface Finishes

Having discovered that we could obtain a uniform, non-filamenting discharge in the region between two parallel aluminum plates, that the laser output power was only a little lower than what we could obtain with the channel waveguides, and that we could obtain single mode operation with relative ease, we decided to make a parametric study of this geometry in addition to simply comparing surface finishes.

We expect from simple waveguide theory[1] that the optical propagation coefficient (in dB/meter) should increase as the inverse cube of the separation between the parallel plates. The small-signal gain, on the other hand, should increase linearly with the inverse separation. Eventually the waveguide loss will overcome the gain and the performance should suffer. And the fixed losses (mirror absorption, output coupling fraction) do not change with the plate separation (to first order; there are second order effects caused by diffraction in the short space separating the mirrors from the ends of the guide.) Just where the waveguide loss becomes the dominating factor was not known initially, since we had only theoretical estimates for that loss.

We undertook a series of experiments with metal plates 20 mm by 370 mm, a considerably wider laser than the two-channel laser, which was about 5 mm by 370 mm. The mirrors used for these experiments had 99.5% reflectivity for the feedback mirror, and 90% reflectivity for the output coupler. Both mirrors were flat. The first set of metal plates were evaluated just as they came from a standard milling machine. We estimate the surface roughness for those plates as 2 micrometers rms. The results are shown in Fig. 20, with the power output plotted vs gas fill pressure (using our standard mix of CO_2:N_2:He of 1:1:6) with the plate separation as a parameter. We were not able to reach the optimum pressure point, limited by our r-f drive power to about 1 kW at 146 MHz. Clearly, the smaller separations prefer higher pressures, as we would expect from "pd = constant" scaling laws for glow discharges. And we see that down to separations of 1 mm, we were able to maintain the same maximum output power, indicating that the waveguide losses aren't increasing too rapidly. Below about 1 mm separation, there is a serious falloff in power. We think this is evidence that the waveguide losses are comparable to the mirror and end-

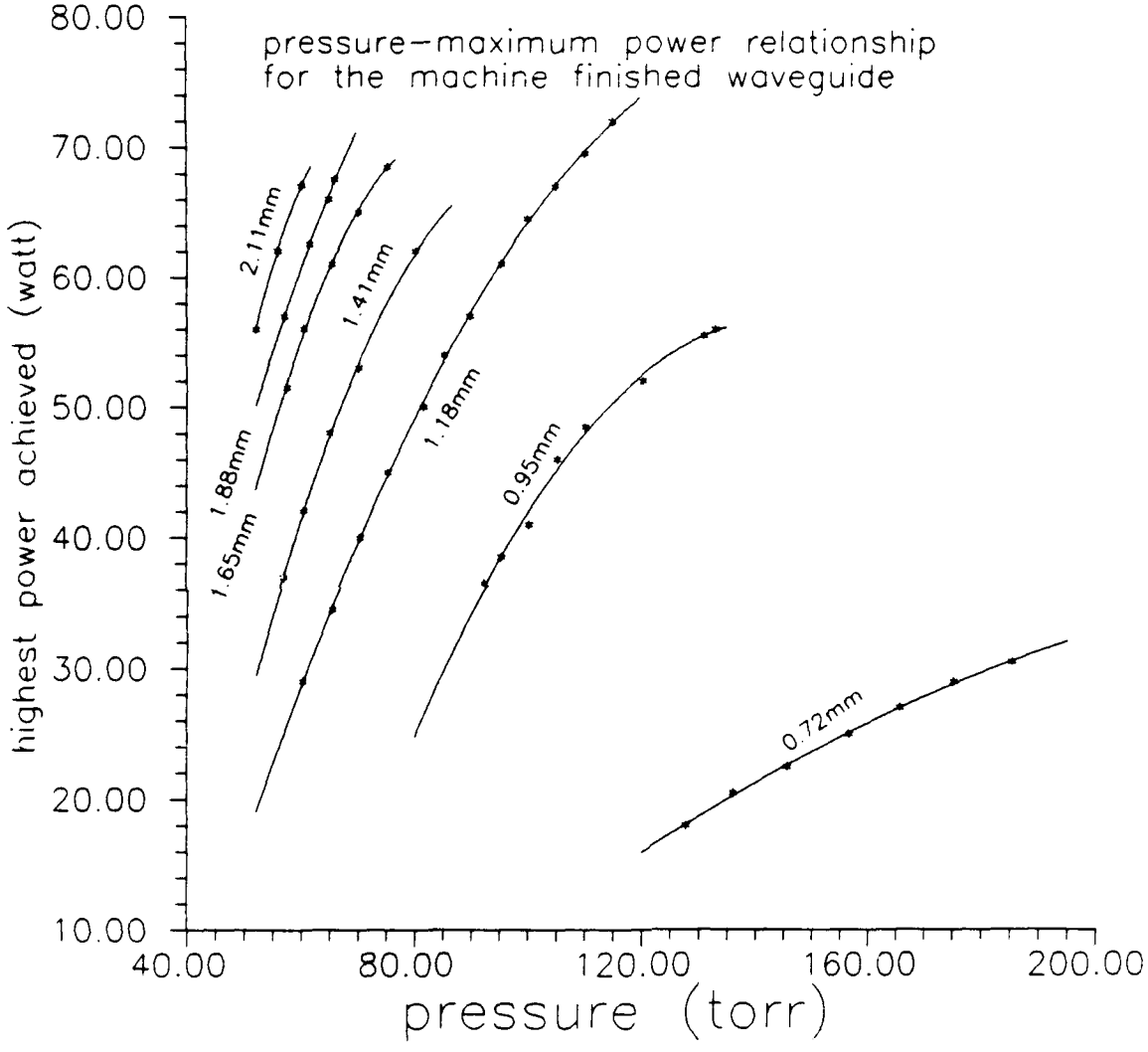

Fig. 20 Pressure-maximum power relationship for the milling machine surface finish, with rms roughness of about 2 μm. An apparent power drop occurs at a gap range between 1.18 mm to 0.95 mm.

diffraction losses at about that spacing, and then increase rapidly as the inverse cube at smaller spacings.

Figure 21 shows a similar set of curves taken with a pair of aluminum plates that were roughened with sandpaper after being machined. We estimate the surface roughness for these as 9 micrometers rms. We note that these curves are not much different from those of Fig. 20, maybe just a little worse. Figure 22 shows another similar set of curves, taken with aluminum plates polished by an outside firm [Jancur Gauge Co.] that claimed a finish with 0.1 micrometers rms roughness. Figure 23 shows another set taken with as-milled plates that had been anodized with a coating thickness of 5 micrometers Al_2O_3. From Figure 3 we would estimate that this coating would *increase* the loss by a factor of 50 from bare aluminum for the TE modes, assuming, of course, that our "bare aluminum" samples had little or no natural oxide layers. However, the curves with the anodized coatings are not significantly different from the others. All these curves are surprisingly similar in performance, indicating that neither surface finish nor material finish is of first-order performance in determining the operating parameters. We have plotted samples of all four finishes in Fig. 24 for comparison. Unfortunately, we were not able to reproduce the glass spacer thickness accurately from one set of plates to another, so the plate spacings are not exactly the same; nevertheless, no clear advantage of one finish over the other is evident from Fig. 24. We should note that the laser output was polarized parallel to the waveguide plates (TE) in all cases.

Since there seems little choice between the finishes studied, it would seem that we would be able to recommend the cheapest (as-milled) and an anodized finish to reduce discharge erosion of the plates (since they are also the discharge electrodes and suffer ion bombardment) and reduce chemical clean-up of the discharge oxygen (from dissociated CO_2) by oxidizing a bare metal surface.

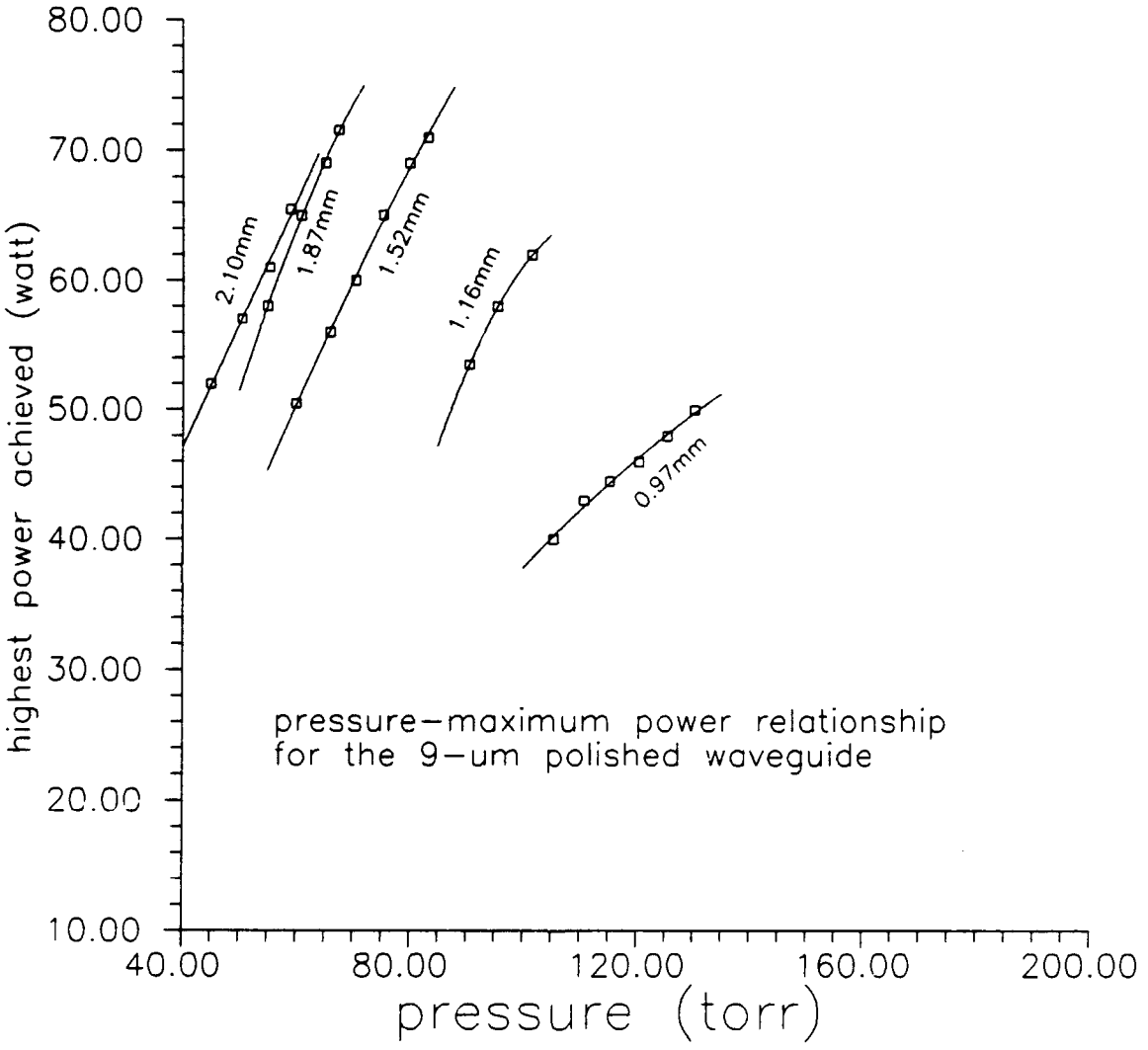

Fig. 21 Pressure-maximum power relationship for the 9 μm surface finish. The power drop occurs at a gap size of around 1.16 mm.

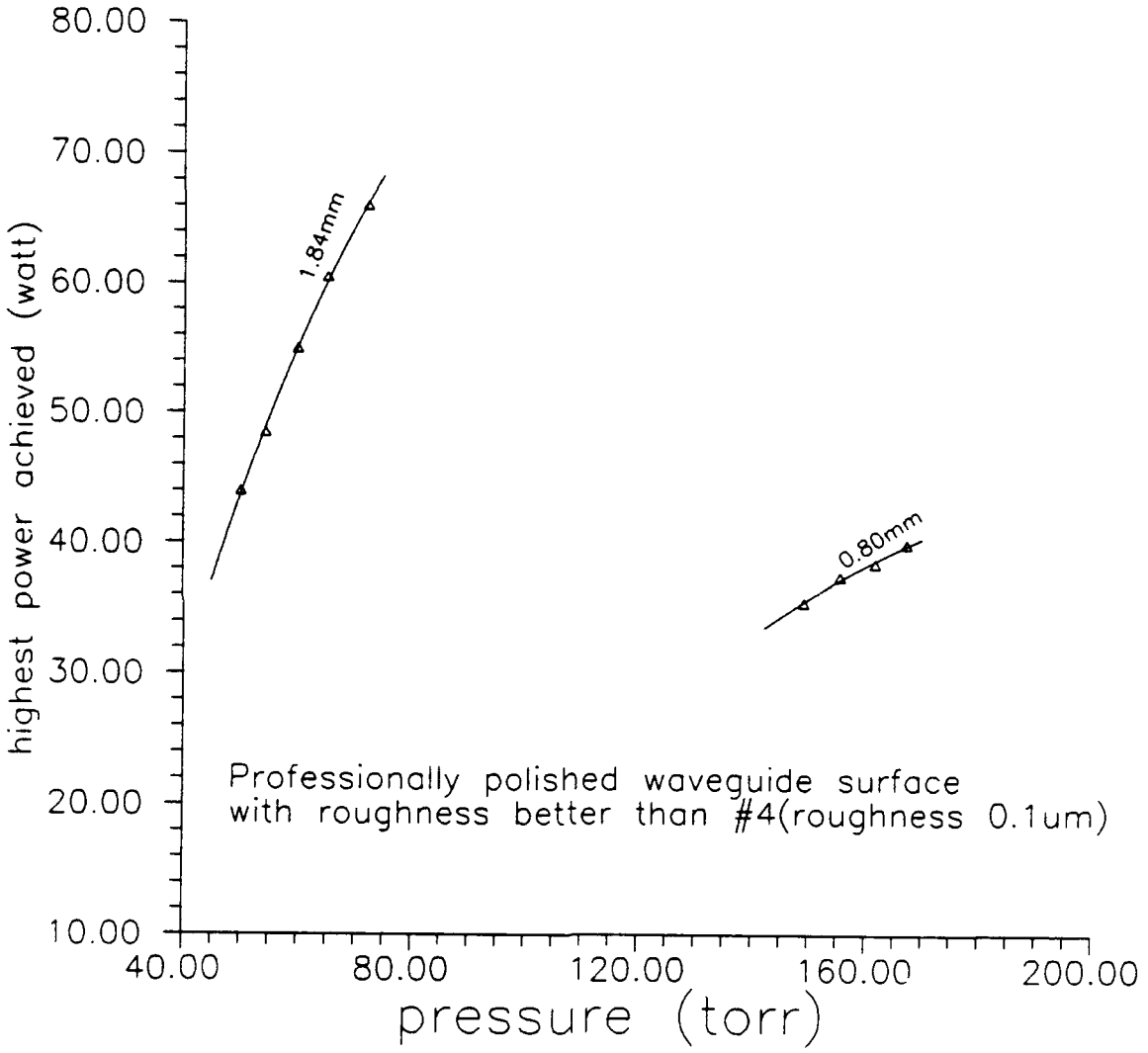

Fig. 22 Pressure-maximum power relationship for a pair of professionally polished waveguide surface with a rms roughness around 0.1 μm. Power drop similar to that in Fig. 20 and Fig. 21 is seen.

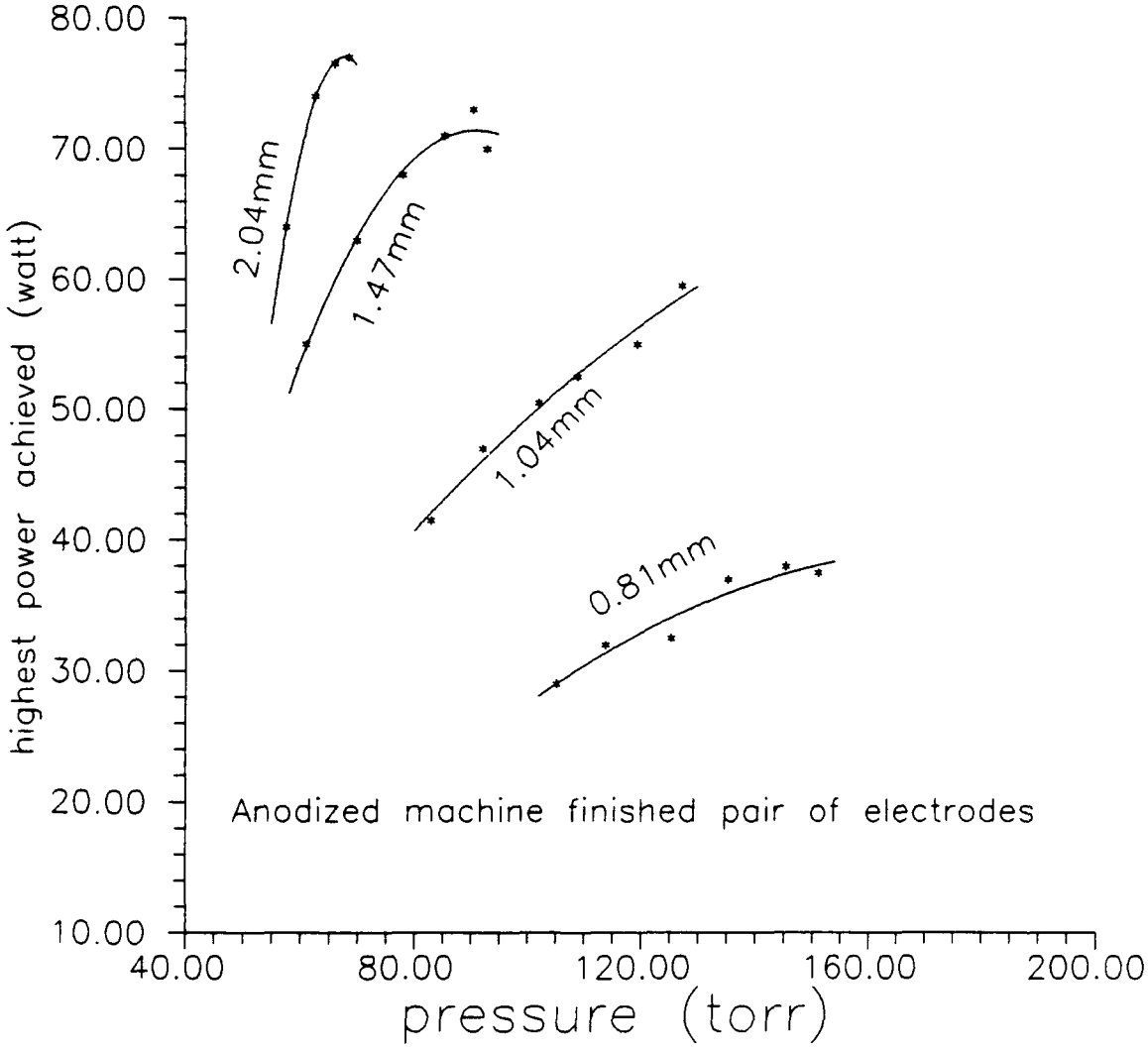

Fig. 23 Pressure-maximum power relationship for the anodized milling machine surface finish, rms roughness is about 2 μm. Power drop is again similar to Figs. 20 - 22 as the gap is reduced.

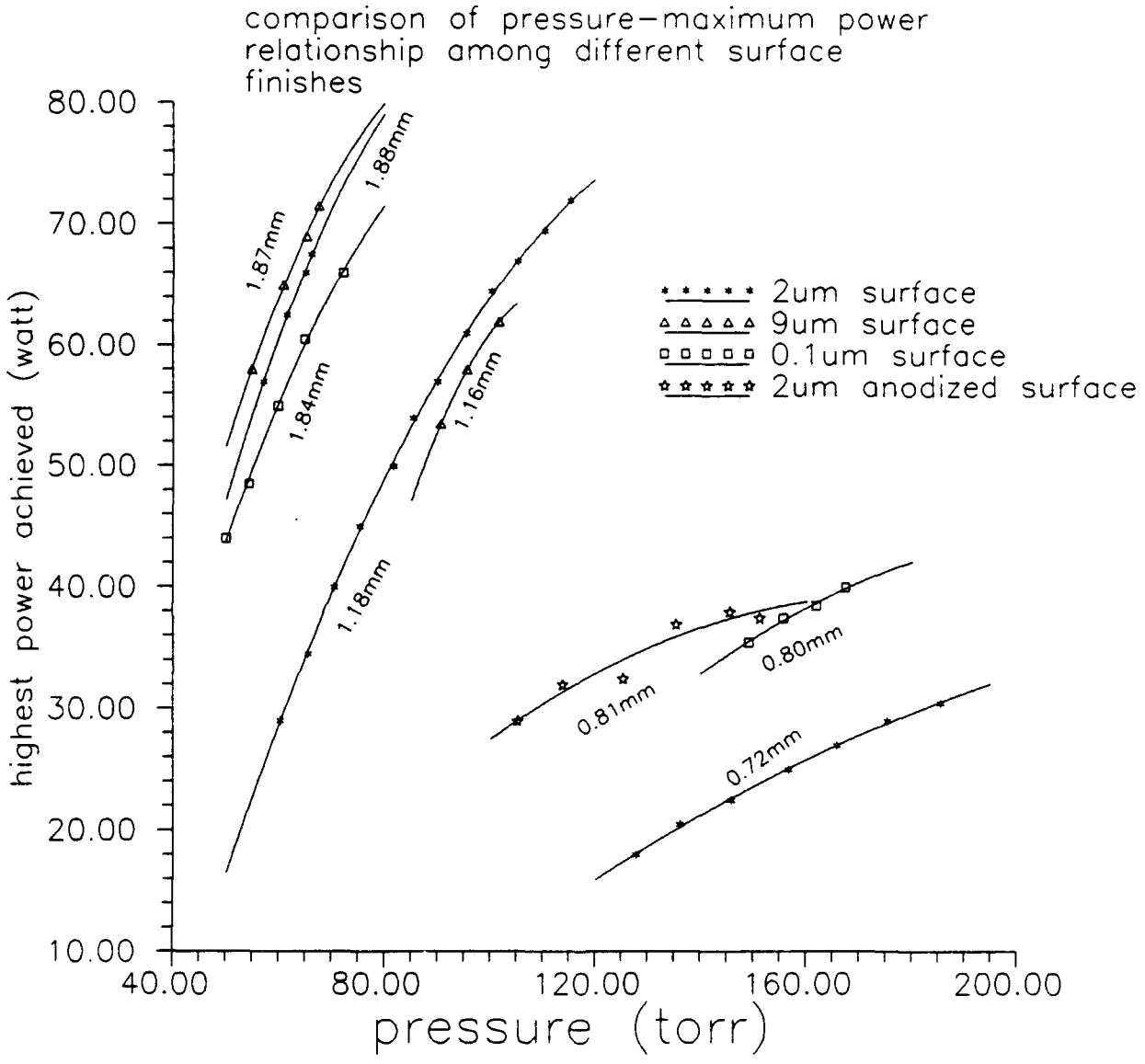

Fig. 24 A comparison of the pressure-maximum power relationship among different surface finishes. It is seen that although there are some differences, the general trend is the same.

2. Calculation of Laser Power at Different Gap Sizes.

All the above measurements indicate that the guide loss of the slab waveguide plays a major roll only when the gap is small, less than 2 mm. Simple laser oscillation theory shows this: For steady state oscillation of the laser, the total gain of the homogeneously broadened medium must be equal to the total loss:

$$\gamma = \frac{\gamma_0}{1+\frac{I}{I_s}} = L, \tag{1}$$

where γ_0 is the small signal gain, I_s is the saturation intensity, which increases with the pressure quadratically. L is the loss coefficient and can be partitioned as follows: (see Fig. 25.)

$$L = L_g + L_d + L_{mr} \tag{2}$$

The waveguide loss coefficient is:

$$L_g = c_g \frac{2\lambda^2}{a^3} Re\left[\frac{1}{\sqrt{n^2-1}}\right], \tag{3}$$

where λ is the laser wavelength, a is the gap size, and n is the complex index of refraction for the waveguide material, and c_g is a coefficient we introduced to include the enhancement of the loss by the surface roughness.

L_d is the loss due to diffraction when the light goes out from the waveguide and is reflected back by the mirrors. We use the Fraunhofer diffraction as an approximation to estimate the diffraction angle:

$$\theta = 2.44\frac{\lambda}{a}, \tag{4}$$

and the area that is missed after the light is reflected back from the mirror. The lost light should be proportional to the relative area that missed the waveguide. Because the sinusoidal distribution of the field across the gap, the power lost should be less than that in the case of uniform distribution. Thus L_d is written as:

$$L_d = c_d \frac{h\,\theta}{a+h\,\theta}\,\frac{1}{L} \qquad (5)$$

where c_d is the correction factor that is less than 1 to account for the fact that the laser distribution is not uniform, h is the distance from the end of the waveguide to the mirror, L is the length of the waveguide.

L_m is the mirror loss, including both that due to the output (T) and that due to the absorption (A_b) at the mirror surfaces:

$$L_m = -\ln\,[\,1-T-A_b\,]\,\frac{1}{2L}. \qquad (6)$$

The intensity inside the cavity is considered to be the sum of the intensities of the two traveling waves in opposite directions, so the output laser power P_o is related to the intra-cavity intensity I by:

$$P_o = 0.5\,ATI, \qquad (7)$$

where A is the area of the laser beam cross-section. This in combination with the laser gain equation yields:

$$P_o(a,p) = 0.5sp^2T\,[\frac{\gamma_0}{L(a)}-1], \qquad (8)$$

where a stands for the gap size and p for the pressure. From our measurements, it was found that pa = 12~13[cmtorr], so we take p12.5/a in the calculation.

Table 1 lists the numbers chosen for the calculation:

TABLE 1 PARAMETERS FOR POWER CALCULATION

Parameter	Value	Unit	Reference
L	38.1	cm	actual value
γ_o	0.08	cm^{-1}	mid-range Ref. 2
T	0.1		actual value
Ab	0.02		estimate
n	27.7 - i94		Ref. 13
c_g	varies		taken as parameter
c_d	0.1		estimate
λ	0.00106	cm	actual value
s	0.3	$watt/(cm)^2$	chosen to fit curve

a)

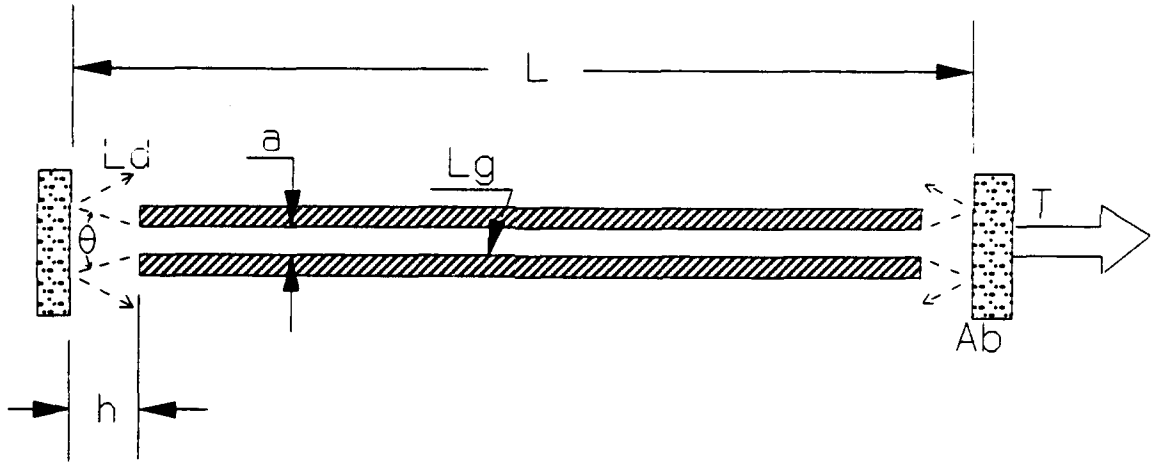

b)

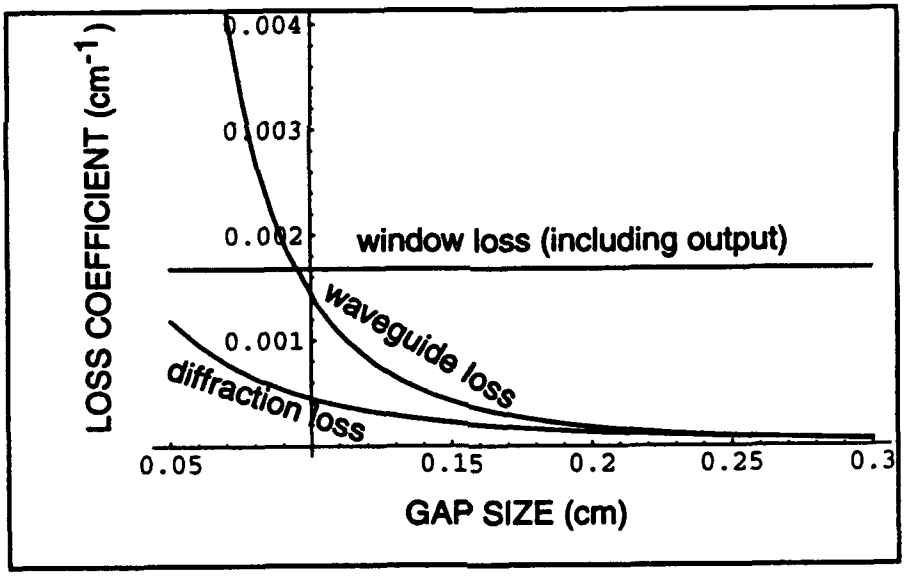

Fig. 25 a) Schematics showing various loss mechanisms; b) Comparison of the losses over a range of gap size. The sum of the waveguide loss and the diffraction loss becomes comparable to the output loss at around 1 mm.

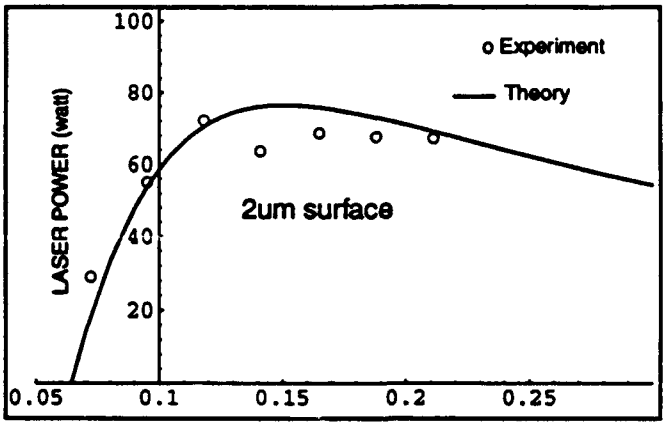

(a)

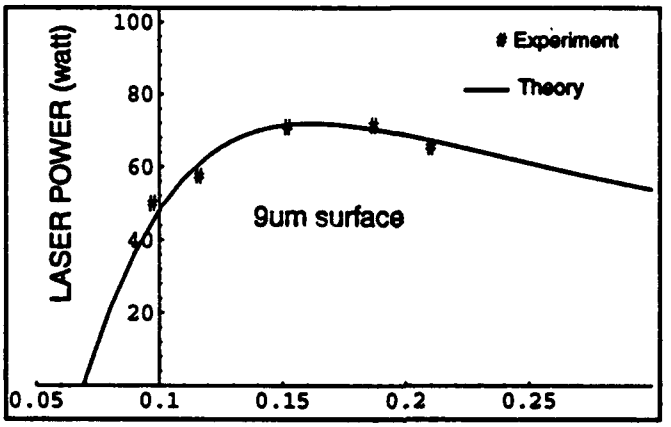

(b)

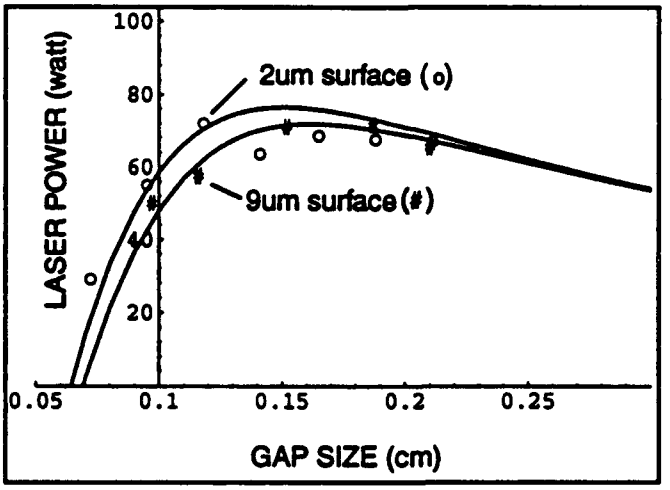

(c)

Fig. 26 The optimum power output as a function of the waveguide gap size. Good agreement with experimental results on two different surface finishes is seen. (a) $c_g = 220$; (b) $c_g = 280$; (c) a comparison between the two surface finishes.

B. MODE COUPLING OF STRIP WAVEGUIDES WITH SLOTS

1. Basic Idea.

Our success with these simple parallel-plate guides, coupled with the continued frustration in obtaining all-in-phase operation of the coupled channel waveguides caused us to consider how we might obtain good mode control in such a slab structure. We knew that we could use unstable resonators, but we also conceived of a new and fundamentally different method of obtaining an all-in-phase output from a slab waveguide. A patent has been applied for (see the section on patents and publications) and a talk given on the technique[14].

Perhaps the easiest way to explain the new idea is by contrast with the problem of supermode selection in the coupled channel arrays. As we discussed in the Section E of the REVIEW, the simple physical reason that the out-of-phase supermode of the array dominates over the in-phase supermode is that the out-of-phase mode has nulls positioned at the separating wall, while the in-phase mode has a finite value at the separating wall, and thus suffers a proportionately higher loss than the out-of-phase mode because of the shadowing of that portion of the mode by the wall. (See Fig. 15) By contrast, a situation that would favor the in-phase mode over the out-of-phase mode would be one in which there is *gain* rather than loss at the coupling wall. Then the in-phase mode, with its finite amplitude, would benefit from that gain more than the out-of-phase mode, with its null. While we were working with the coupled channel guides, we considered how we might arrange this, but could think of no simple way to accomplish it. However, the slab guide provided the answer: Here is a situation where there is gain *uniformly* across the width of the array. The in-phase mode is naturally preferred over the out-of-phase mode.

Of course there are a couple of small problems. First, the slab geometry no longer has walls between the channels, so that the individual waveguides we are trying to couple are no longer defined! We considered leaving very small walls to define the channels, but any obscuration at all would introduce more loss in the in-phase mode than the out-of-phase mode. Second, once the walls are removed, the Gaussian-cosine modes can also oscillate, and they do, as we demonstrated in Fig. 19. What we really need is a structure that will suppress the Gaussian-cosine modes without introducing loss in the space between the channels. The solution to this problem is to put *grooves* in the waveguide walls, introducing significant waveguide loss for the Gaussian modes. The nulls in a higher order Gaussian mode are not equally spaced

across the width of the mode, and furthermore, they do not follow straight lines from one end of the guide to another; they form hyperbolas. (See ref. 15, for example.) Thus, introducing straight slots in the waveguide walls will suppress the Gaussian-cosine modes. And these slots also define the waveguide channels for a coupled-channel system, but they do so as "negative walls" that introduce no loss in the region above the slots.

Figure 27 (a) shows the new geometry, compared with the wall-coupled channels (b), and the simple slab waveguide (c). We have built experimental versions of this idea, with individual channels of 2 to 5 mm width, and with slots in one plate 1 to 2 mm wide and 2 mm deep. (We could have also put slots in both plates, but the configuration shown in Fig. 27 (a) seems to work just fine.) We have operated the laser with waveguide spacings of 0.9 to 1.4 mm, in order to have a discharge that occurs primarily between the "lands" and the other wall, with little discharge in the region above the slot. This makes a better definition of where the "channels" are and where the "walls" are. However, there may still be some small gain in the visibly "dark" region over the slots. This would enhance the preference for the in-phase mode over the out-of-phase mode, as long as it isn't large enough to encourage the Gaussian-cosine modes. If the wall-to-land spacing is made too small, the discharge fills the width more or less uniformly, and the mode control suffers. Likewise, if the slots are made too thin, the discharge fills in and mode discrimination again suffers. Note that this structure is all metal, with as-milled finishes in the guiding portion. The r-f matching network for this structure is essentially the same as the plain slab guides; the interplate capacitance is changed very little, as is the discharge loading.

2. Experimental Results

Stable in-phase operation was obtained in two and five-channel array lasers. (The two channel laser performed better in output power, likely because we had neither the r-f power to excite the larger area of the five-channel guide nor the cooling capacity to handle the higher power required.) We undertook to test the "robustness" of this mode control scheme in the same fashion we used in the coupled channel guides. We introduced intentional losses by placing three pieces of glass upright in the slots and extending across the guide, as shown in Fig. 28 (a). These obstacles introduce a significant shadow loss in the in-phase mode, and when we did the similar test in coupled channel waveguide, repeated here in Fig. 28 (b), we completely suppressed the in-phase mode. We found that we needed to introduce three glass pieces

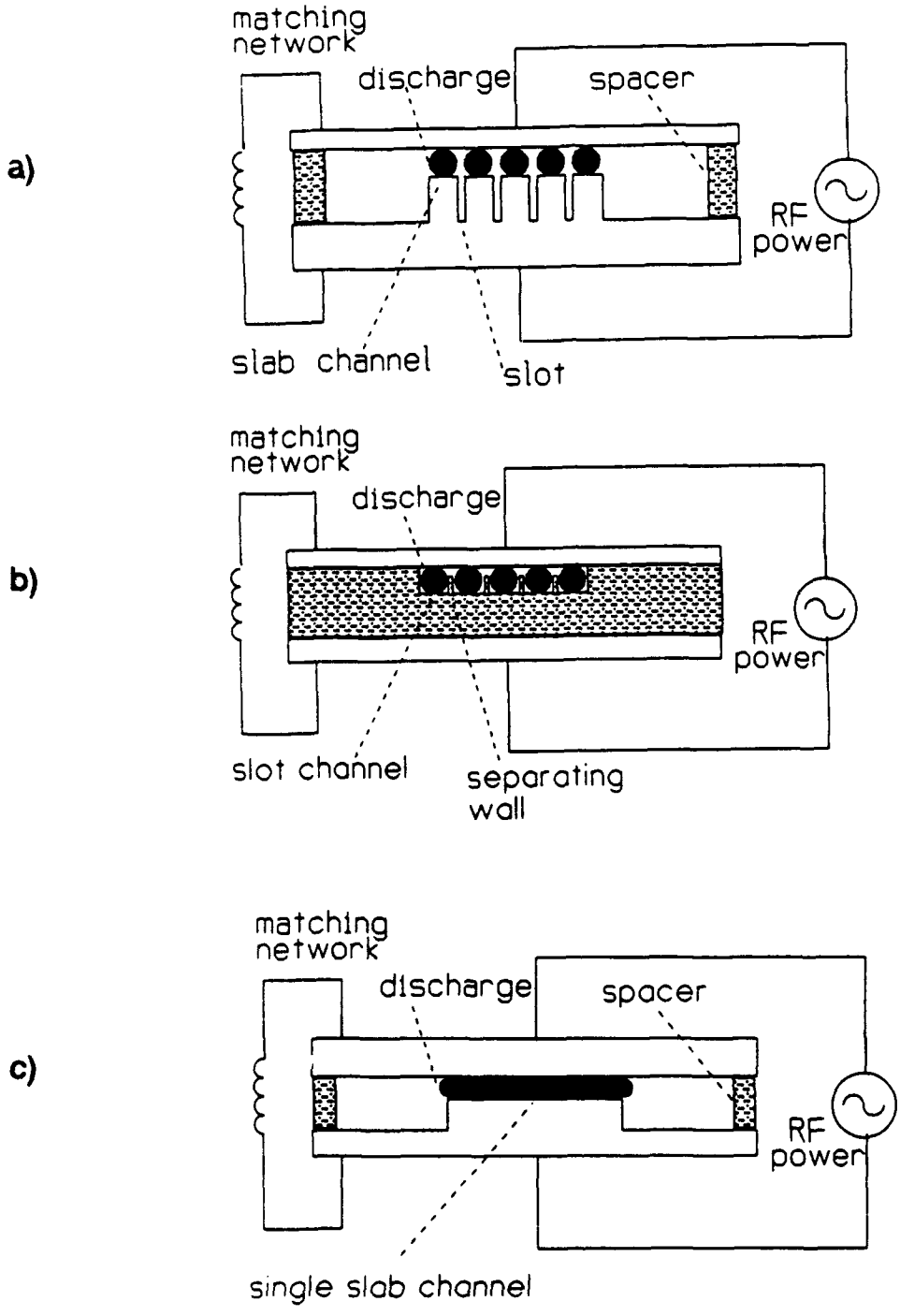

Fig. 27 Illustration of the slot coupled array and comparison with previous structures. a) Slot coupled waveguide array, b) Wall coupled waveguide array, c) Single slab waveguide laser.

distributed along the guide as shown in Fig. 28 (a) to even see the out-of-phase mode, and even then, operation drifted back into the in-phase mode asthe temperature changed. This showed that the out-of-phase mode is unstable while the in-phase coupled mode is stable. The selection of the in-phase mode is quite robust in the slot array.

Figure 29 shows a scan of the far field pattern of a five-channel slotted waveguide array. There is one central lobe and two symmetric side lobes down 6 dB. Figure 30 shows the evolution of the burn patterns on lucite for a two channel slotted waveguide array. A telescope was formed from lenses f_1 and f_2, forming a focal spot 15" from f_2. A series of burn patterns were taken at distances 7" to 15" from lens f_2 at 11" intervals; as shown in Fig. 30. The near field shows the two individual channels and the far field exhibits a strong central lobe with weaker side lobes.

As we stated above, if the slots are too thin, or the spacing between the plates is too narrow with respect to the channel width, we lose the suppression of the Gaussian-cosine modes. Figure 31 shows the results of an unsuccessful design and its corresponding mode pattern (observed on a thermal imaging plate) which looks suspiciously Gaussian! Note that there are four lobes with three nulls from an array with three channels and two slots. Clearly, the mode is "ignoring" the slots entirely. Of course, we need more than good mode control in a practical laser; we also need good output power and good efficiency. Figure 32 shows the output power of a two-channel slotted array (curve ending in M) which was operating in a stable in-phase mode. Also shown is the multimode output power from a slab guide of the same overall width and spacing (curve ending in Q). The multimode slab has more output, but at the high end the single mode, slotted waveguide has 73% of the multimode slab guide, not a bad comparison for single mode versus multi-mode. It is likely that an unstable resonator mode selection scheme might also reduce the power by a similar amount. The curve ending in P is the same data as Q, but scaled by the "land" area to overall width of the slotted guide, to represent a slab guide of the same wall area. In that comparison, the slotted wall guide is only 13% lower power than the scaled slab guide.

Figure 33 shows the mode spectrum of the slab guide Q described above. A clear single beat note was observed, showing that the output was not only in a higher order mode, but there was more than one mode. The slotted wall array M exhibited no such beat notes, indicating true single mode operation.

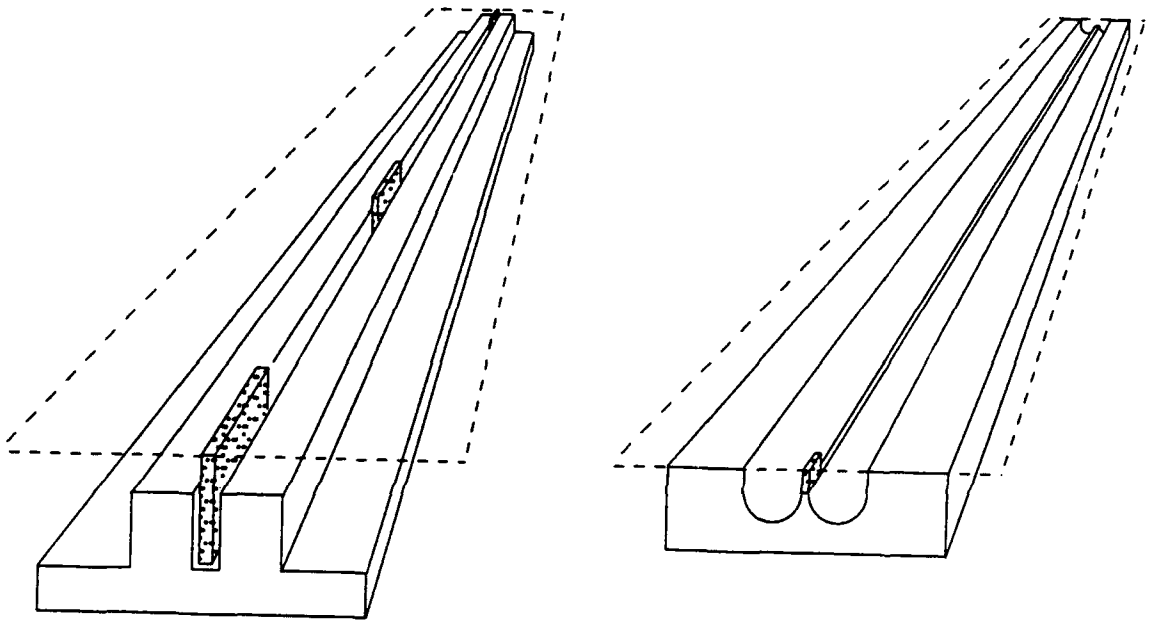

Fig. 28 a) The slot coupled array. The intentional loss introduced in the coupling region produced only a short-lived out-of-phase coupled mode. The stable mode was still the in-phase coupled mode. b) Wall coupled array. The same type of lossy material, with less total loss than the case of a), caused the in-phase coupled mode to disappear completely; only the out-of-phase mode could be obtained.

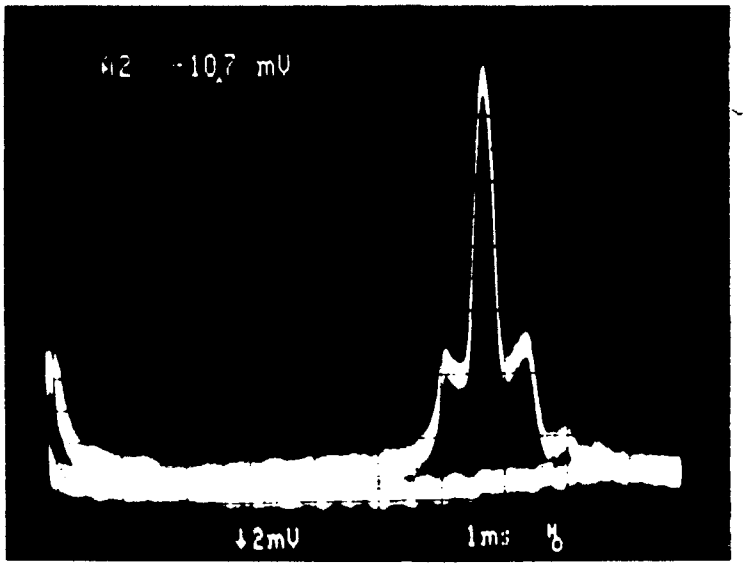

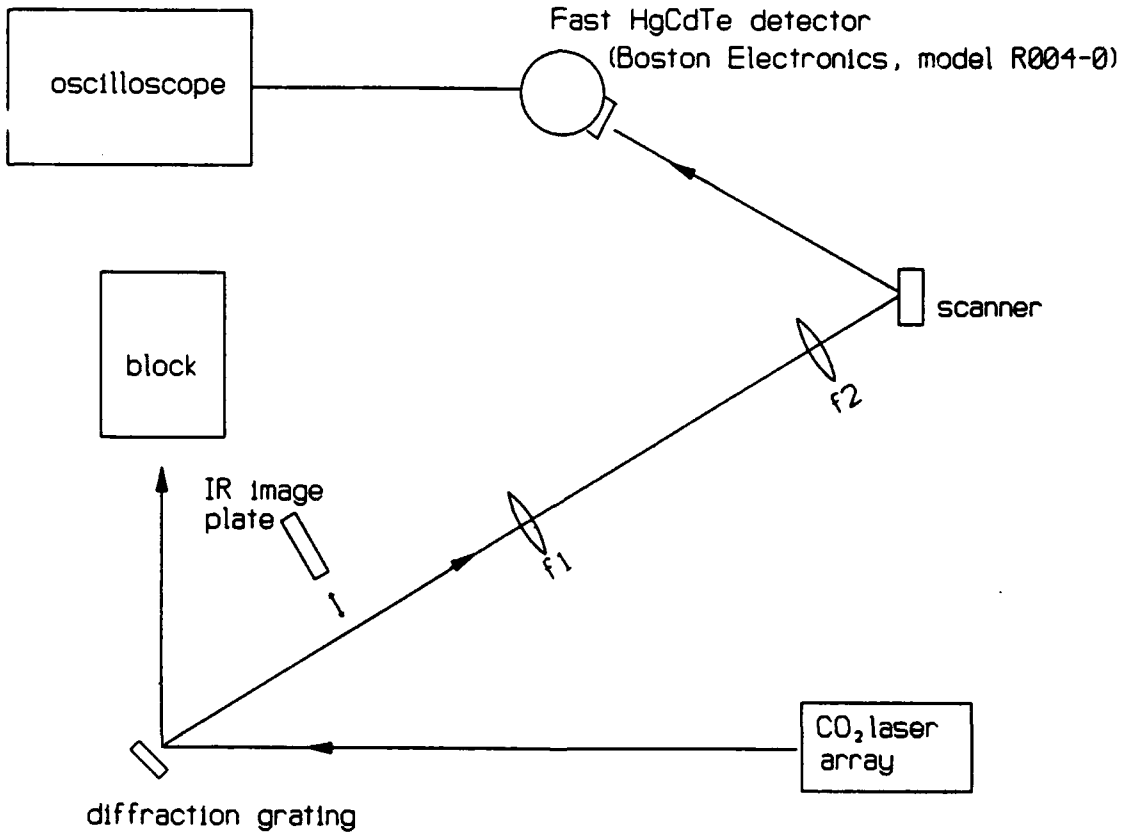

Fig. 29 Far field scan of a five-channel, slot-coupled waveguide array output and the measurement setup.

a)

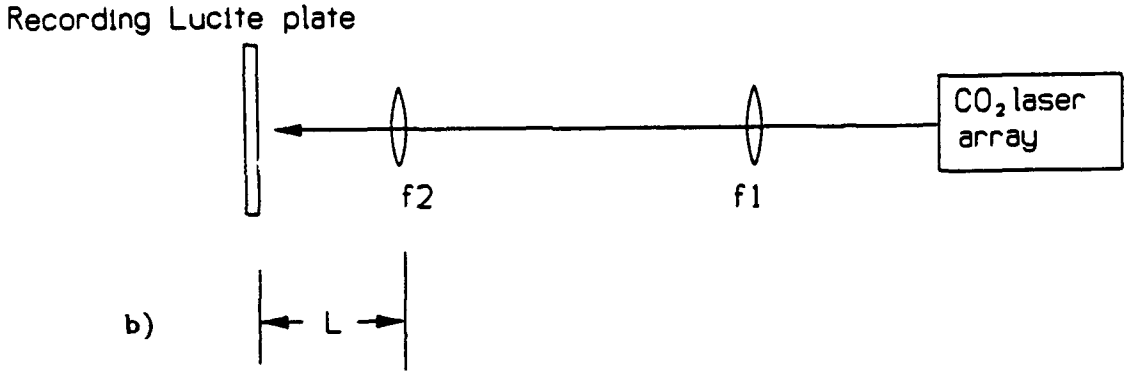

Fig. 30 The evolution of the power distribution from near field to far field: a) the patterns were burnt at increasing distances from the focusing telescope $f_1 + f_2$. b) the measurement layout.

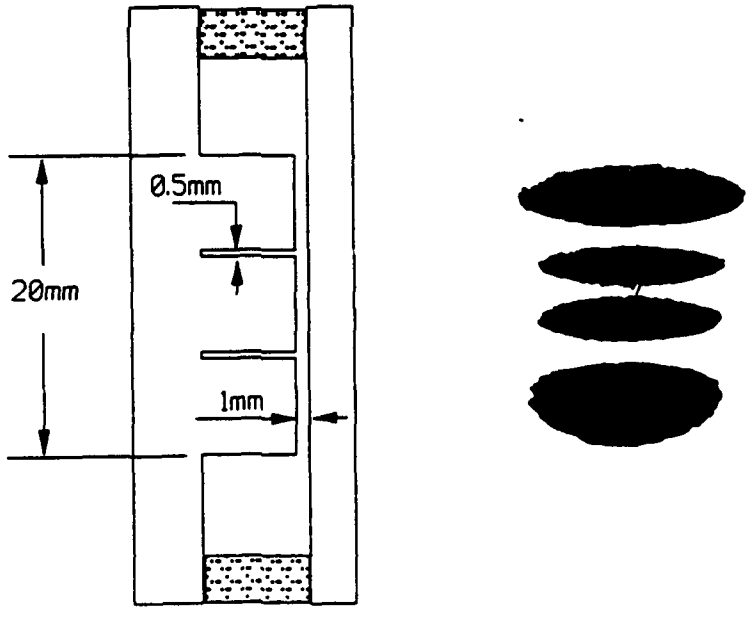

Fig. 31 An unsuccessful structure failed to cut the wide slab waveguide into individual small waveguides. The near field pattern is characteristic of a single slab waveguide.

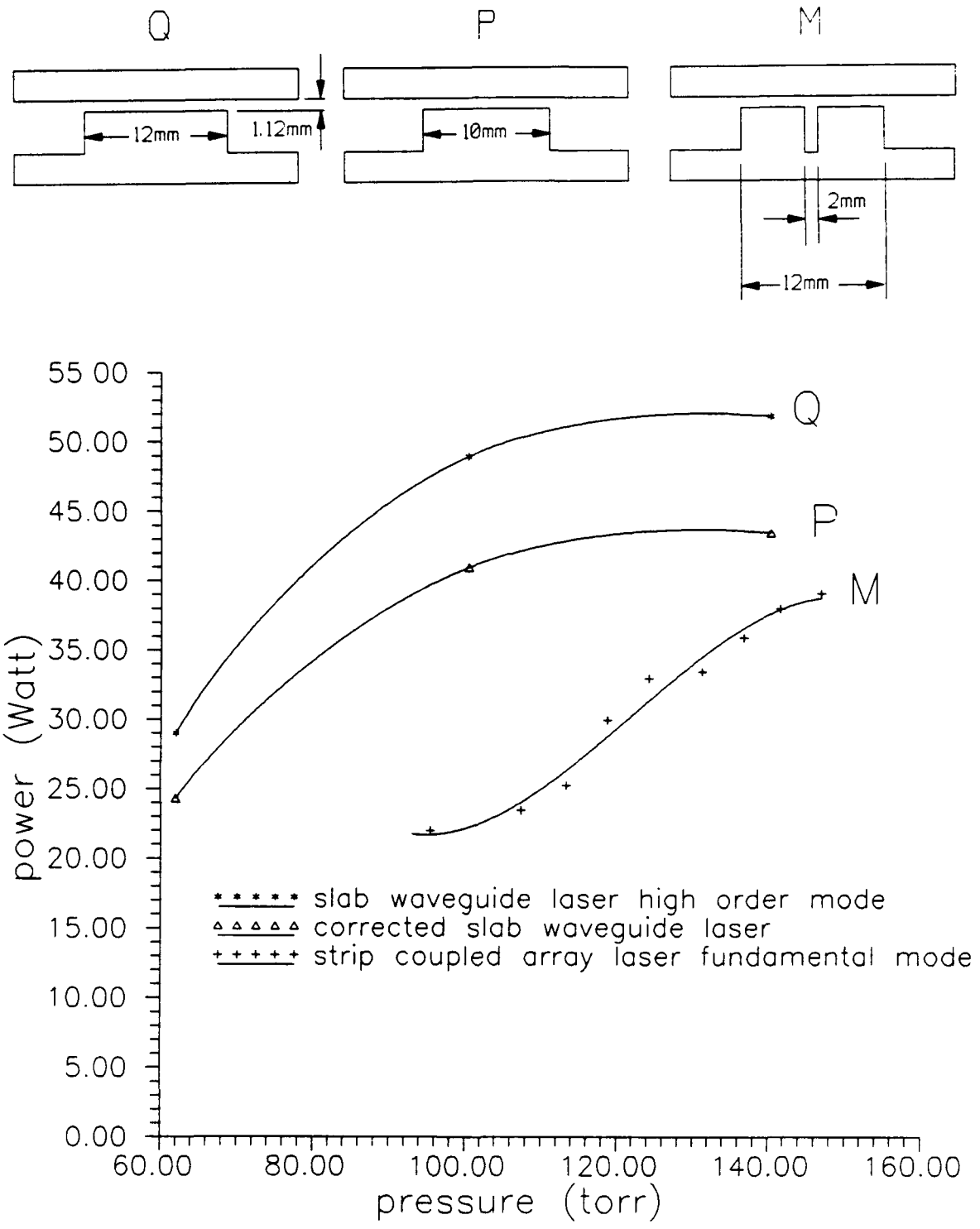

Fig. 32 Output power comparison between the strip array laser and slab laser. Curve M is for the slot-coupled strip array. Curve Q is for the slab with the same overall volume as the strip array. Curve P is for a slab reduced in volume so that it has the same slab surface area as the sum of the area for the ridges in the strip array. The reduction in power is assumed to be in proportion to the reduction in area. The maximum power point M is 73% of Q and 87% of P.

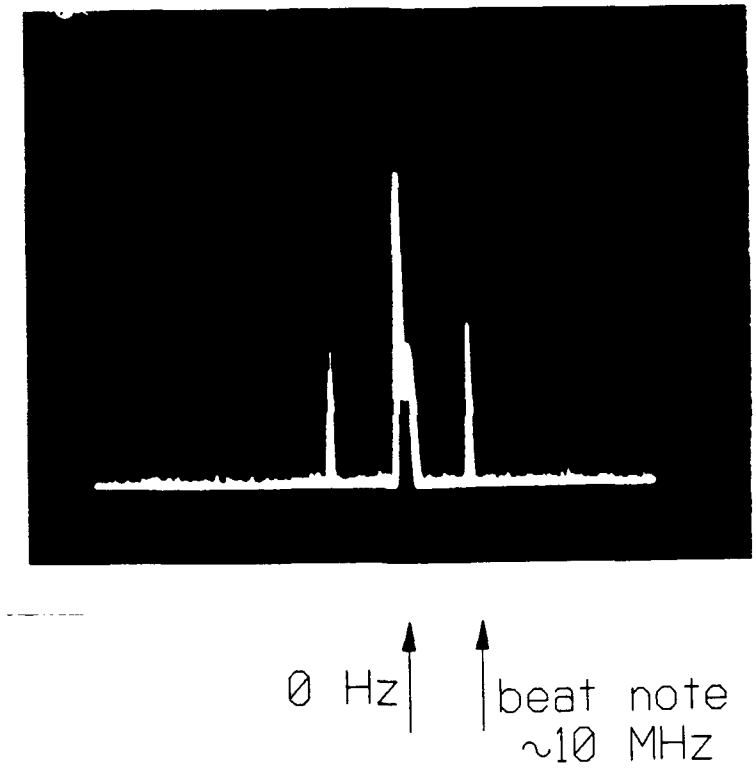

Fig. 33 The beating notes for the slab waveguide laser (Q in Fig. 32). No such beating was observed in the corresponding coupled strip array (M in Fig. 22) when the cavity alignment is adjusted correctly.

C. MICROWAVE-EXCITED, ALL-METAL, PLANAR WAVEGUIDE LASER

1. Basic Concepts

Our demonstration of bare metal slab waveguide walls lead us to consider how we might make an *all metal* waveguide laser of much simpler construction and excited by a much less expensive power source. Figure 34 illustrates the evolution of our reasoning. Figure 34a shows the transverse cross section of the waveguide and vacuum structure used in our test-bed laser. The two metal slabs forming the optical waveguide are separated by insulating spacers, and also joined by inductors to form a resonant LC circuit at 146 MHz. The entire assembly is suspended inside an external metal vacuum chamber. The r-f excitation is brought into the vacuum chamber via a vacuum-tight coaxial feedthrough insulator. All waveguide lasers demonstrated to date that we know of utilize similar elements. The separation of the vacuum envelope from the waveguide walls is necessitated by the need for an insulating spacer between the waveguide walls, which also serve as the r-f electrodes. Either the separate vacuum chamber shown is required, or a continuous, vacuum tight, metal-to-insulator seal at the edges of the slab would be required, a difficult task to contemplate, and one not demonstrated as far as we can determine.

However, if the resonating inductor could be made in the form of a vacuum-tight connecting metal wall, as shown in Fig 34b, there would be no need for the insulating spacer, and the electodes/optical waveguide plus this inductive wall could form the outer vacuum envelope of the laser. Of course, such a wall would have much lower inductance then the coils or straps used in our experiments (and by other workers), so that the resonant frequency would be increased greatly. We normally think of a power source becoming more expensive as its frequency increases. However, there is an "anomalously low" cost associated with microwave power at 2450 MHz, the frequency used by commercial microwave ovens. A 750 Watt output magnetron, with greater than 75% efficiency can be purchased for $60 retail. The whole oven... sheet metal, controls, fan, power supply, controls, and magnetron, retails for $150 - $300. Thus we were motivated to consider what dimensions would be suitable for this frequency.

The structure illustrated in Fig 34b is actually referred to in the microwave literature as a double ridge-loaded waveguide, and is often used to decrease the transverse dimensions of a standard waveguide. As we propose to use it, the ridge surfaces form both the optical waveguide and the r-f waveguide for

(a)

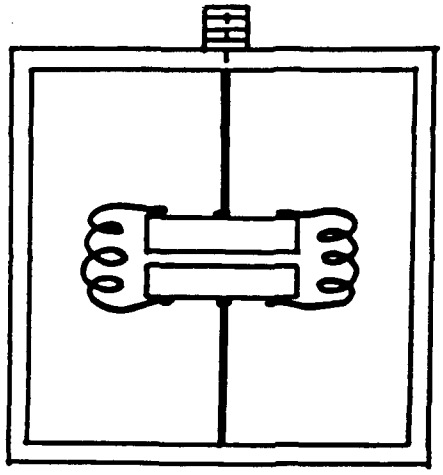

(b)

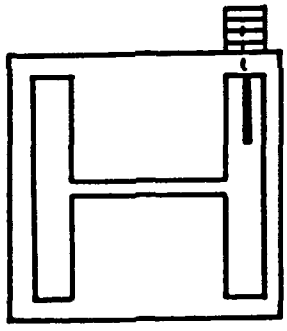

Fig. 34 (a) Cross section of LC resonant slab laser inside a vacuum chamber, similar to the test bed laser used in this project. One side is grounded and the other is fed with r-f at 146 MHz through a hermetically sealed coaxial fitting. (b) Cross section of a double ridge-loaded waveguide, with dimensions just above cutoff frequency at 2450 MHz. R-f coupling is shown schematically here as a probe antenna attached to a hermetically sealed coax connector.

the pump power. Strong electric field concentrations occur between the opposing surfaces of the ridge, so that this structure is not often used with high power microwave systems, since an r-f discharge would be inclined to break down in this field-concentration region. However, that is just what we desire to happen here: We want to form a discharge primarily between the ridges to form the active region of our laser. Any discharge should concentrate here if we adjust the ridge spacing and the gas pressure to favor a Paschen minimum in that region, and that gas pressure is already approximately the laser operating pressure.

The other dimensions of the waveguide are not arbitrary. The waveguide must be big enough so that microwaves propagate, that is, the waveguide must not be seriously cut off. However, reflections from the open-circuited ends of the slabs will cause a microwave standing wave to form, and that would lead to non-uniform excitation of the plasma. (In fact, standing waves are somewhat of a problem at 146 MHz.) The free-space wavelength at 2450 MHz is 122.5 mm, significantly shorter than the overall length of the laser that we wish to realize. As the waveguide transverse dimensions are adjusted toward the cutoff condition, the guide wavelength increases over the free-space wavelength, and becomes infinite exactly at the cutoff conditions. Thus, to make a long laser, the transverse guide dimensions should be adjusted to be near cutoff, but just a little larger. As a practical matter, the loading by the discharge will change things, so we chose to calculate the exact cutoff dimensions, and then determine the actual optimum conditions by experiment.

2. Ridge Waveguide Theory

There is no exact electromagnetic field solution for the ridge waveguides shown in Fig. 35. Various approximate solutions have been published by Cohn[15] and Chen[16]. We chose to use the technique developed by Cohn[15], which treats the guide as a *propagating structure in the transverse direction.* The condition for cut off of the longitudinal guide is when this transverse propagating system is an integral number of its guide wavelengths long; that is, when it is in resonance. The model treats the ridge region as one parallel plate line and the "inductor loop" as another, shorted parallel plate line. The step discontinuity where these two lines meat is treated by adding a lumped "discontinuity capacitance" to the transmission system, as calculated by Whinnery and Jamieson[17]. The dimensions of the the transverse cross section are then varied to obtain the resonant condition.

We have computed a set of curves showing these dimensions parametrically for the single ridge waveguide, as shown in Fig. 36. We find that we can make a reasonable single ridge waveguide, just cut off at 2450 MHz, with a gap spacing of 2.8 mm and a ridge width of 15 mm, and that, further has an overall rectangular dimensions of a standard copper microwave waveguide, WR-137, so that we could fabricate a test vehicle without undue machining. This cross section is shown in Fig. 37. Note that WR-137 guide is cut off at 4301 MHz with the ridge absent. Thus, to obtain "short circuit" sections at the ends of the waveguide to confine the fields we need only to end the ridge, just in front of the optical mirrors. It turns out that offsetting the ridge can be used as a fine adjustment to the resonant condition; a completely symmetrical structure is probably desirable in the end, but would necessitate actually machining the structure to specific dimensions, rather than using commercial copper waveguide.

Unfortunately, the present contract expired as we were beginning to consider this approach. We were unable to perform any experiments, even during the no-cost extension to 30 June 1991. However, we continue to pursue the idea, albeit in fits and starts, as we shall describe our results and plans in the EPILOGUE.

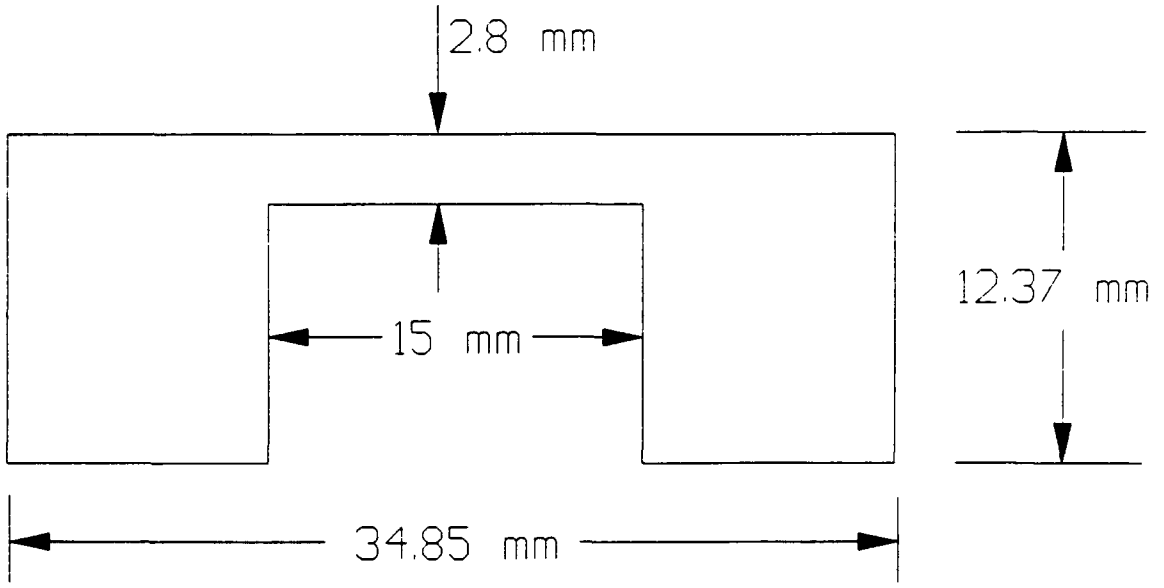

(a)

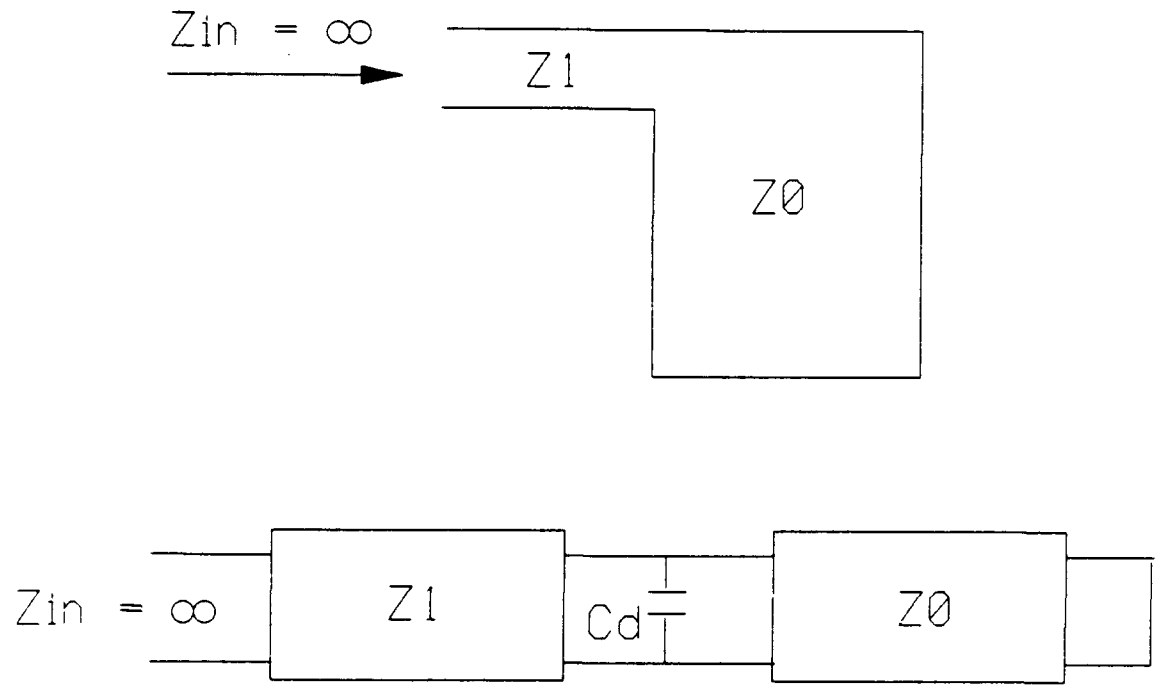

(b)

Fig. 35 (a) Single ridge waveguide and (b) Its equivalent transmission line circuit for the lowest order mode.

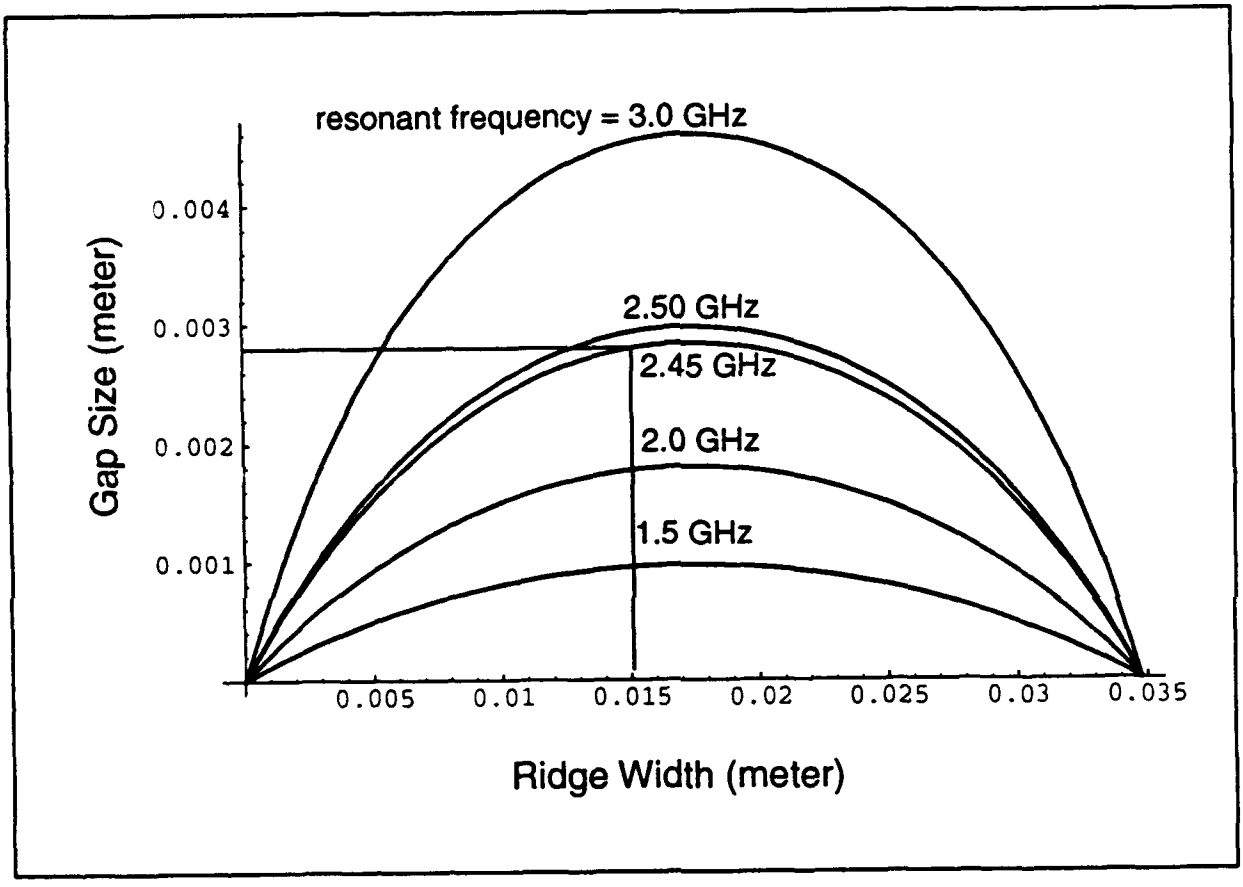

Fig. 36 *Cutoff conditions for the single ridge waveguide made from a standard* **WR-137 waveguide (34.8 x 12.4 mm^2). A 15 mm wide ridge and a 2.8 mm gap makes the waveguide cutoff at 2450 MHz.**

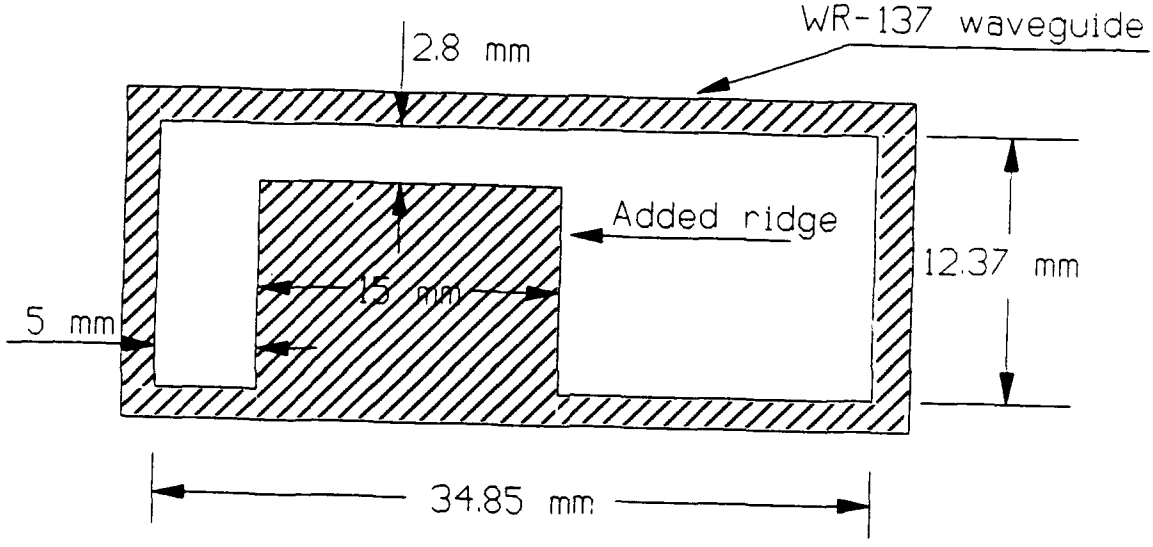

Fig. 37 The final experimental ridge waveguide. Shifting the ridge off the waveguide center helps compensate for the discrepancy between theory and practice.

EPILOGUE

A. POST CONTRACT RESULTS

As stated in the previous section, the present AFOSR contract ended before we were able to make significant progress on the all-metal, microwave-excited slab waveguide laser concept. We continued working with Caltech funding while we sought support from other sources. We submitted a proposal for joint funding from the Hughes Aircraft Company (1/3) and the State of California Office of Competitive Technology (Comptech) (2/3), and were told we were successful. Unfortunately, Comptech's portion was withdrawn, dissappearing into the black hole of California's FY92 budget deficit. We did receive $30,000 from Hughes, and made some further progress in the late summer and fall of 1991. In March 1992, Comptech informed us that their budget had been partially restored, and we should "requalify" our project. Again, we were told we were successful, but we are still awaiting a contract (while another black hole develops in California's FY93 budget!) However, we continue to work (slowly) with Caltech funds.

Since June, 1991, we have built a ridge waveguide structure of the dimensions shown in Fig. 37, and confirmed that it is near cutoff at 2450 MHz by probing the field distribution to measure the guide wavelength. We salvaged a 2450 MHz magnetron and power supply from a defunct microwave oven and successfully coupled the magnetron to standard S-band WR-284 waveguide. WR-284 is a little small for 2450 MHz operation; Japanese standard "oven waveguide" is somewhat larger, but we had access to waveguide sections, tuners, directional couplers, etc. in WR-284, so we chose to use it rather than build everything we needed to the "oven waveguide" standards. We built a well-matched, high-power water calorimeter in WR-284 guide and measured the output power of the magnetron. We ordered a commercial WR-284 waveguide vacuum window (thin, aperture matched) and used it in our initial experiments to try to feed power to our preliminary ridge waveguide structure in an r-f hot test. Figure 38 is a photograph of the hot-test discharge section (extreme left) coupled to the magnetron via a "three screw" tuner and pressure window as it appeared in our first tests. Unfortunately, this window burned out rapidly when a discharge formed at the surface of the window, a result of contamination from a down-stream arc that occurred while trying to match at high power. We have sucessfully built our own "half-wave" window from a large piece of polystyrene inside a section of WR-284 guide; it is much more robust, having survived several matching mishaps.

Fig. 38 Ridge waveguide hot test setup built after the end of the present contract. The ridge waveguide is at the extreme left. It is aperture-coupled to the WR-284 waveguide at the center. A three-screw tuner and pressure window (with flange sandwich) are also used. The magnetron hangs below the waveguide (the soda can is only used to provide scale in the photograph.) The microwave oven power supply components have been reassembled on a breadboard, with the Varian providing power controls.

The status of our experiments as of May 1992 is that we are developing a match into the ridge waveguide discharge structure by cut and try.

B. FUTURE PLANS

We will continue our experiments on the microwave-pumped waveguide laser until we are successful or until our resources are exhausted. If we are successful, we will attempt to incorporate the slot coupled array concept into the slab, to obtain an all-in-phase array with simple plane mirrors, as an alternative to using an unstable resonator on the simple slab waveguides.

PERSONNEL

The Principal Investigator for this program was Professor William B. Bridges, who devoted 20% of his time to the project and was directly involved in all phases of the work.

Mr. Yongfang Zhang joined the project in June, 1988 as a graduate research assistant. Mr. Zhang has a B.S. degree in physics from Northwest University, Xian (1982) and a M.S. degree in physics from Huazhong University of Science and Technology, Wuhan (1984.) At HUST, Mr. Zhang was involved in research on optics for high power CO_2 lasers and served as an instructor and quantum electronics project advisor for seniors. He spent a year at Fairleigh Dickinson University as a visiting scholar and a year in graduate studies at the University of New Mexico. He is currently a candidate for the Ph.D. degree in Electrical Engineering at Caltech, anticipated June 1993.

Mr. Reynold E. Johnson has contributed to this project as engineer on a part-time basis. Mr. Johnson joined the staff of Caltech in 1989 after his retirement (early) from the Hughes Aircraft, where he worked for 23 years. Mr. Johnson has worked in microwaves, semiconductor devices, and lasers at the Hughes *Research Laboratories as Senior Associate Engineer.* He transferred to the Hughes Missile Systems Group in 1981, in retired in 1988 as a Development Engineer Specialist.

INTERACTIONS

The early phases of this program were helped greatly by interactions with Mr. Richard A. Hart of UTOS. Mr. Hart was helpful both in loaning us ceramic waveguide array sections that he had used in his setup at UTOS, and in the general advice in laser characteristics and r-f matching they had observed at UTOS. This kind of informal industry - university interaction should be encouraged, since both parties benefit from the interchange of somewhat differing viewpoints. University personnel become aware of the practical limitations and goals of the industrial projects, and industrial personnel are exposed to a wider range of scientific questions and "side-alleys" that the industrial atmosphere tends to suppress.

In September 1989, Professor Bridges attended QE-9, the British National Quantum Electronics Conference, held at Oxford that year. Several papers on waveguide lasers were presented by Professor Denis Hall of Heriot-Watt

University, Edinburgh, and his students, and by scientists from the Royal Signals and Radar Establishment. Professor Bridges also visited Professor Hall's laboratory at Heriot-Watt in early October for a discussion of waveguide laser research. On his return from Europe, Bridges visited UTOS in West Palm Beach, Florida for fruitful discussions with Mr. Richard A. Hart on the waveguide laser array work at UTOS.

Both Bridges and Zhang attended CO_2 laser sessions at CLEO '90 in Anaheim, California, and LASERS '90 in San Diego. Mr. Zhang attended LEOS '91 and gave a paper (see next section) and LASERS '91.

Although they occurred after the official end of this contract, we include the following for general information: Our ideas on microwave-discharge-excited, all-metal waveguide CO_2 lasers were discussed with Dr. Michael Henderson of the Electro-optical and Data Systems Group of the Hughes Aircraft Company. As a result, we received promise of a small support grant from Hughes, and a joint proposal to the State of California Office of Competitive Technology (CompTech) for double matching funds. We were successful in receiving an award, but the State Legislature withdrew CompTech's funds for FY91. We are just now negotiating with CompTech for FY92 funds. Meanwhile, the Hughes support allowed us to make some small progress through the Summer and Fall of 1991.

PUBLICATIONS AND PATENTS

There have been no journal publications to date. A paper covering the slot mode control was presented at the 1991 Annual Meeting of the Optical Society of America by Mr. Zhang: "Stable In-Phase Locked Array of CO_2 Waveguide Lasers" by Yongfang Zhang and William B. Bridges.

The patent disclosure written before the start date of the contract on the "striped mirror" concept of in-phase mode extraction issued during the contract period: William B. Bridges, "Coupled Waveguide Laser Array," U.S. Patent No. 4,884,282, assigned to the California Institute of Technology.

Although not part of this program, the basic patent on the gap-coupled waveguide laser array also issued during the contract period: A.J. DeMaria and William B. Bridges, "Dielectric Ridge Waveguide Gas Laser Apparatus," U.S. Patent No. 4,813,052, assigned to the United States of America as represented by the Secretary of the Air Force.

A disclosure on the slot mode control concept was filed on 6 August 1991: Yongfang Zhang, "In-Phase Coupled Strip Waveguide CO_2 Laser Array," and has been assigned serial number 07740973 by the U. S. Patent Office.

A disclosure on the microwave wave excited all metal concept was sent to the Caltech patent office and has been assigned number 92-1, rated for filing and awaits drafting.

REFERENCES

1. W.B. Bridges and Y. Zhang, "Coupled Waveguide Gas Laser Research," California Institute of Technology, Annual Report on Grant AFOSR-88-0085, May 31, 1989.

2. R.L. Abrams and W.B. Bridges, "Characteristics of Sealed-Off Waveguide CO_2 Lasers," IEEE Journal of Quantum Electronics, Vol. QE-9(9), pp. 940-946, September, 1973.

3. E.A.J. Marcatili and R.A. Schmeltzer, "Hollow Metallic and Dielectric Waveguides for Long Distance Optical Transmission and Lasers," Bell System Technical Journal, Vol. 43, pp. 1783-1809, July 1964.

4. K.D. Laakmann and W.H. Steier, "Waveguides: Characteristic Modes of Hollow Rectangular Dielectric Waveguides," Applied Optics, Vol. 15, pp 1334-1340, May 1976. *Errata*, Applied Optics, Vol. 15, p. 2029, September, 1976.

5. D.V. Willets and C. Hartwright, "An Anodized Aluminum Waveguide CO_2 Laser," J. Phys. D: Appl. Phys., Vol. 11, pp. L111-L114, 1978.

6. Synrad Advertising, brochure received October, 1991.

7. M. Miyagi and S. Nishida, "Transmission Characteristics of Dielectric Tube Leaky Waveguide," IEEE Transactions on Microwave Theory and Techniques, Vol. MTT-28(6), pp. 536-541, June 1980.

8. M. Miyagi A. Hongo and S. Kawakami, "Transmission Characteristics of Dielectric-Coated Metallic Waveguide for Infrared Transmission: Slab Waveguide Model," IEEE Journal of Quantum Electronics, Vol. QE-19(2), pp. 136-145, February 1983.

9. M. Miyagi, Y. Wagatsuma, A. Hongo and S. Nishida, "Output Power Characteristics of Thin Film-Coated Waveguide CO_2 Lasers," Optics Communications, Vol 61(3), pp. 229-232, February 1987.

10. A. Yariv and P. Yeh, Optical Waves in Crystals, John Wiley and Sons, P. 487, 1984.

11. B. Adam and F. Kneubühl, "Transversely Excited 337 μm HCN Waveguide Laser," Applied Physics, Vol. 8, pp. 281-291, December 1975.

12. L.A. Newman, A.J. Cantor, R.A. Hart, J.T. Kennedy, and A.J. DeMaria, "Coupled High Power Waveguide Laser Research," Final Report on Contract F49620-84-C-0062, July 30, 1985.

13. Handbook of Optical Constants of Solid State Materials, Academic Press, Inc., E.D. Palik, editor, 1985.

14. Y. Zhang and W.B. Bridges, "Stable In-phase Locked Array of CO_2 Waveguide Lasers," THJ5, Optical Society of America 1991 Annual Meeting, Nov. 3-8, 1991, San Jose, California.

15. S.B. Cohn, "Properties of Ridge Wave Guide," Proc. IRE, Vol. 35, pp. 783-788, August 1947.

16. T. Chen, "Calculation of the Parameters of Ridge Waveguides," IRE Transactions of Microwave Theory and Techniques, Vol. MTT-5, pp. 12-17, January 1957.

17. J.R. Whinnery and H.W. Jamieson, "Equivalent Circuits for Discontinuities in Transmission Lines," Proc. IRE, Vol. 32, pp. 98-116, February 1944.